ELSEVIER

Coordination Chemistry Reviews 236 (2003) 121–141

COORDINATION CHEMISTRY REVIEWS

www.elsevier.com/locate/ccr

Communication between iron(II) building blocks in cooperative spin transition phenomena

José A. Real [a,*], Ana B. Gaspar [a], Virginie Niel [a], M. Carmen Muñoz [b]

[a] *Departament de Química Inorgánica/Institut de Ciencia Molecular, Facultat de Química de la Universitat de València, Dr. Moliner 50, 46100 Burjassot, València, Spain*

[b] *Departament de Física Aplicada, Universitat Politécnica de València, Camino de Vera s/n, 46071 València, Spain*

Received 3 April 2002; accepted 30 August 2002

Contents

Abstract . . . 121
1. Introduction . . . 122
2. Intermolecular interactions in mononuclear $[Fe(L)_2(NCS)_2]$ spin crossover complexes where L = bipy, btz, phen, and dpp . . . 122
   2.1 Magnetic properties and character of the spin conversion . . . 123
   2.2 Intramolecular changes upon spin conversion . . . 123
   2.3 Molecular packing and cooperativity . . . 124
   2.4 Thermal dilatation and compressibility studies on single crystals . . . 125
      2.4.1 Thermal dilation data . . . 125
      2.4.2 Compressibility data . . . 126
   2.5 Concluding remarks . . . 128
3. 2,2′-Bipyrimidine bridged iron(II) dinuclear spin crossover complexes . . . 129
   3.1 Structural characterisation . . . 129
   3.2 Magnetic properties . . . 129
   3.3 Influence of pressure dependence on the thermal variation of the magnetic susceptibility . . . 130
   3.4 Photo-switching between spin pairs . . . 131
4. Polymeric spin crossover compounds . . . 131
   4.1 One-dimensional coordination polymers . . . 131
   4.2 Two-dimensional coordination polymers . . . 134
   4.3 Three-dimensional coordination polymers . . . 137
5. Conclusion and outlook . . . 138
Acknowledgements . . . 140
References . . . 140

Abstract

In the present article we discuss the cooperative nature of the spin crossover phenomenon in iron(II) complexes, providing a perspective of the state of the art in this area. The first aspect we discuss is the role of the intermolecular interactions, more precisely the π-interactions, in mononuclear complexes. We show that by playing with the nature of the ligands, aliphatic, aromatic, or extended aromatic, it is possible to create stronger cohesive forces and receive a more cooperative response from the compound. In the next step the singular family of bipyrimidine-bridged iron(II) dinuclear compounds is presented as the simplest example of polynuclear spin crossover complexes exhibiting a rich variety of magnetic behaviours, which stem from the synergistic effect between intramolecular and cooperative intermolecular interactions. Finally, a number of polymeric 1-3D architectures of varying dimensionality and topology are discussed in terms of the search for strong cooperative spin crossover systems.

Keywords: Molecular magnetism; Spin transition; Iron(II) complexes; Supramolecular chemistry

* Corresponding author. Tel.: +34-96-398-3001; fax: +34-96-386-4322
E-mail address: jose.a.real@uv.es (J.A. Real).

0010-8545/02/$ - see front matter
PII: S0010-8545(02)00220-5

1. Introduction

Functional materials based on molecular building blocks represent an increasingly important area of research in contemporary chemistry [1]. For instance, switchable molecules can occur in two different long-lived states. Switching between two states may induce drastic changes in chemical and physical properties of the molecules, and hence of the material, which can eventually undergo a phase transition [2]. Changes in properties at the transition phase are often of technological interest, and several materials applications of phase transitions have been found [3].

Six-coordinate Fe(II) spin crossover compounds represent an important class of switchable molecular systems [4,5]. For these compounds the energy gap between the fundamental diamagnetic low-spin (LS) state and the excited paramagnetic high-spin (HS) state is close to thermal energy. Then, a spin-state conversion can be driven by an external input of information such as a gradient of temperature or pressure, and by light irradiation. The reversible spin conversion involves the transfer of two electrons between the t_{2g} and e_g orbitals. Consequently, a change in the magnetic and optical properties of the compound can be observed. In particular, when the molecules have no charge transfer absorption bands in the visible region, a dramatic change of colour takes place upon spin conversion. The intra-ionic electron transfer is concomitant with a variation of the iron-to-ligand bond distance being 0.2 Å greater in the HS state [6]. This change of molecular size is transmitted cooperatively from one site to another in the crystal via intermolecular interactions. Cooperativity is one of the most appealing and elusive concepts in spin crossover phenomena. The nature of the interactions has been a subject of discussion for physicists and theoreticians for more than 30 years and continues to be a source of interest, as can be inferred from two recent papers by Spiering and Hauser et al. [7,8]. Based on the elasticity theory Spiering et al. have demonstrated that the elastic interactions, stemming from the change in volume of the spin crossover molecule, give rise to long-range contributions. These interactions may be pictured as an internal pressure, which increases with the concentration of the LS species, and interacts with all the molecules in the crystal with the same strength irrespectively of distances [7].

We are not focusing here on the theoretical aspect of the problem, but rather on how to design strongly cooperative spin transition compounds. The cooperative mechanism of the spin crossover compounds can be considered to be well understood in terms of the above mentioned model, however, due to its phenomenological character the key parameters accounting for intermolecular interactions do not reflect the relevance of microscopic details which could help chemists to design molecular systems with prescribed characteristics. In fact, we consider that very general principles have guided synthetic chemistry in search of suitable spin crossover compounds and often trial and error or serendipity have been the sole strategy.

Cooperativity is ubiquitous in Nature, for instance, it plays an important role in the allosteric changes of proteins. The structural switch of haemoglobin between its active and inactive form is particularly meaningful here as it occurs strongly coupled with the LS-to-HS spin transition in response to the oxygenation–deoxygenation process [9]. Cooperativity is responsible for the dramatic changes observed in the magnetic and optical properties of the spin crossover compounds. As in haemoglobin, the cooperative mechanism strongly depends on the effectiveness of the intermolecular contacts, hydrogen-bonding network, π-stacking, and other specific interatomic interactions, which mediate between the building blocks used to construct the spin crossover compounds.

In the last decade the synthesis and characterisation of new Fe(II) spin crossover compounds has increased considerably. In particular, the structural characterisation of an important number of mononuclear complexes displaying very different cooperative behaviours has been reported. This has made it possible to analyse the cooperative mechanism from a microscopic viewpoint and in some cases to qualitatively rationalise the character of the spin transition through careful investigation of the intermolecular interactions. Most of the information is disseminated in different papers. At the same time new synthetic approaches have been developed in order to explore the cooperative nature of the spin crossover compounds, i.e. replacement of intermolecular interactions by suitable bridging ligands. This approach has afforded a number of dinuclear and polymeric spin crossover compounds with interesting spin crossover behaviours. The present review article is devoted to illustrating strategies we, and others, have developed in order to explore cooperativity from a microscopic viewpoint. Basically, this concept requires the links between the active sites in the crystal to be discovered and the role of these links to be evaluated in terms of the spin crossover regime.

2. Intermolecular interactions in mononuclear $[Fe(L)_2(NCS)_2]$ spin crossover complexes where L = bipy, btz, phen, and dpp

Most iron(II) spin crossover compounds are constituted by mononuclear species with the $[FeN_6]$ coordination core. Among them, the complexes of formula $[Fe(L)_2(NCS)_2]$, where L stands for a bidentate α-diimine ligand, represent one of the most extensively studied families [10–19]. They display a wide range of

spin crossover behaviour from continuous to abrupt conversions even with a large thermal hysteresis loop. In addition, single crystal X-ray studies have been performed for many of these compounds; consequently, correlations between the nature of the spin conversion and the molecular structure and the crystal packing have been performed separately for each compound, giving a very partial view of the problem. In this section we would like to illustrate these correlations highlighting a series of relevant members of this family with L = 2,2′-bipyridine (bipy), 2,2′-bi-4,5-dihydrothiazine (btz), 1,10-phenanthroline (phen) and dipyrido[3,2-a:2′3′-c]phenazine (dpp) (Scheme 1).

2.1. Magnetic properties and character of the spin conversion

Fig. 1 gathers the magnetic response of the four derivatives. The anomalous magnetic properties of compound $[Fe(bipy)_2(NCS)_2]$ were observed by Baker and Bobonich in the 1960s [20] and were confirmed by König and Madeja [21]. This compound undergoes a sharp spin transition at $T_c \approx 213$ K, which can easily be monitored by thermal variation of the product $\chi_M T$ where χ_M is the molar magnetic susceptibility and T is temperature. For temperatures much greater than T_c, $\chi_M T$ remains constant upon cooling down and close to 3.53 cm^3 K mol^{-1}, a value which corresponds to what is expected for an iron(II) ion in the HS state. When the temperature decreases below T_c, $\chi_M T$ drops to 0.4 cm^3 K mol^{-1} (polymorph II), indicating the occurrence of a very cooperative spin transition. More than 75% of the spin change takes place in the range of 4 K. The complete cooling and heating cycle does not indicate the occurrence of thermal hysteresis. It should be mentioned that the residual paramagnetism observed in the LS state of this compound has been found to vary distinctly according to the preparation method in the range 0.1–0.4 cm^3 K mol^{-1}. However, no significant change was observed in the elemental analysis, in the infrared and Mössbauer spectra of the three different isolated polymorphs [22,23].

The compound $[Fe(btz)_2(NCS)_2]$ was first reported by Bradley et al. in 1978 to undergo an incomplete smooth spin equilibrium centred at $T_{1/2} \approx 225$ K ($T_{1/2}$ is the temperature at which the molar fraction of HS and LS molecules is 0.5) [24]. $\chi_M T$ is 2.90 cm^3 K mol^{-1} at 295 K and reaches the lower limit of 0.70 cm^3 K mol^{-1} in the vicinity of 160 K. About 70% of the conversion takes place between 200 and 250 K indicating a continuous character for the spin conversion. However, these values indicate that the spin conversion is not complete either at 295 K or low temperatures.

The compound $[Fe(phen)_2(NCS)_2]$ was also characterised by Baker and Bobonich [20] and by König and Madeja [25]. It exhibits a discontinuous spin crossover in the solid state at a critical temperature $T_c = 176$ K. Like $[Fe(bipy)_2(NCS)_2]$, two different polymorphs have been isolated for the phen derivative. The so-called extracted form (polymorph I) undergoes an almost complete spin transition with a hysteresis loop, ca. 1 K, while the spin transition is less complete, around 16% of molecules remain HS at low temperature, in the precipitated form (polymorph II) (Fig. 1) [26].

The compound $[Fe(dpp)_2(NCS)_2]$py has recently been reported by Zhong et al. [18]. Its magnetic properties show a strong cooperative spin transition with a large hysteresis loop, 40 K width, and T_c equal to 123 and 163 K for the cooling and warming modes, respectively.

In summary, different degrees of cooperativity have been observed in this series of compounds, the btz derivative undergoes a continuous spin conversion whereas the bipy and phen derivatives display discontinuous spin transitions without hysteresis in contrast to $[Fe(dpp)_2(NCS)_2]$py which undergoes a very cooperative transition with a large hysteresis loop.

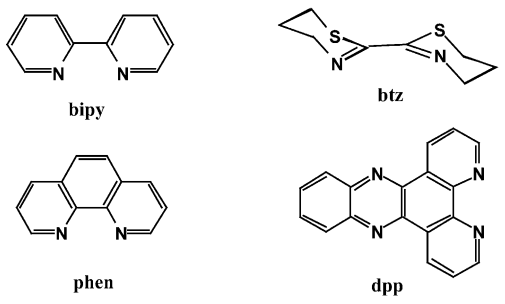

Scheme 1.

2.2. Intramolecular changes upon spin conversion

The crystal structures of $[Fe(L)_2(NCS)_2]$ where L = bipy [11], and phen [10] (polymorphs II) were studied, in the HS and LS states, and it was not until almost 30 years later that the first report of their synthesis appeared. Similarly, the crystal structure of the btz derivative, in the HS and LS states, was reported more than 10 years after its magnetic characterisation [12]. The three compounds remain in the orthorhombic system (space group *Pcbn*) whatever the temperature or pressure may be. Thus, no structural phase transition accompanies the spin change. Their molecular structures are depicted in Fig. 2. Let us recall that the iron(II) ion is surrounded by six nitrogen atoms, the two NCS^- ligands occupy the *cis* conformation and relate to each other, like the L ligands, by a two-fold axis passing through the iron(II) atom. The average Fe–N(L) and Fe–NCS bond lengths for the HS and LS states are in Table 1. The Fe–N bond distances are shorter by ca 0.20 Å for the L ligand and by ca. 0.10 Å for the NCS^- groups upon spin conversion. The distortion of the $[FeN_6]$ core from a regular octahedron is smaller in the

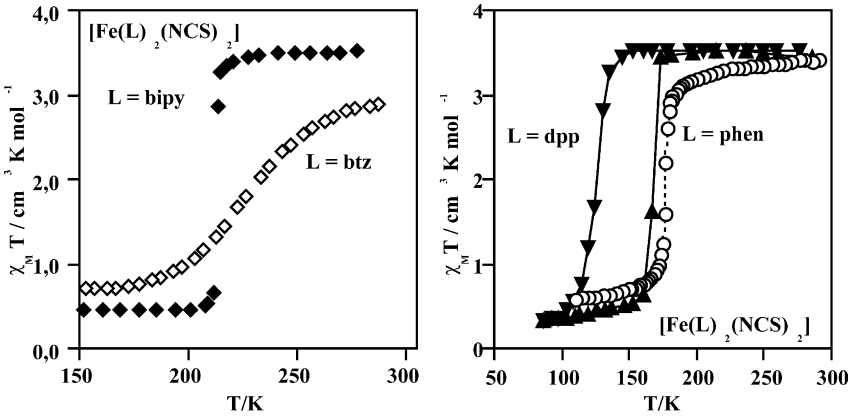

Fig. 1. Magnetic properties of $[Fe(L)_2(NCS)_2]$, (left) L = bipy, and btz, black and white rhombuses respectively, (right) L = phen, and dpp, circles and black triangles, respectively.

LS state than in the HS state. The angle of trigonal distortion $\phi = 60 - \theta$, where θ is defined by three N atoms on the planes perpendicular to the pseudo three-fold axis, is larger for the HS state (14.7–12°) and decreases down to 7.7° in the LS state.

Unlike the precedent $[Fe(L)_2(NCS)_2]$ systems the dpp derivative crystallises in the monoclinic *Pn* space group at room temperature and shows the inclusion of one guest pyridine molecule per complex. Despite these differences, the $[FeN_6]$ chromophore is defined, similarly, by two bidentate dpp ligands and two thiocyanate anions in *cis* position defining a distorted octahedron. The average Fe–NCS bond length, 2.10 Å, is shorter than the average Fe–N(dpp) bond length 2.20 Å (see Fig. 3).

From the structural data it can be inferred that the $[FeN_6]$ chromophore and its changes upon spin conversion are very similar for the four compounds. Consequently, it cannot have any influence on the spin crossover regimes observed for these compounds.

2.3. Molecular packing and cooperativity

As mentioned above, the compounds $[Fe(bipy)_2(NCS)_2]$, $[Fe(btz)_2(NCS)_2]$ and $[Fe(phen)_2(NCS)_2]$ crystallise in the same space group with similar crystal and molecular parameters in the LS and HS states, so that they also display similar crystal packing (Fig. 4). Despite these similarities, their magnetic behaviour differs greatly indicating a big difference in cooperativity.

In the three compounds the crystal packing can be similarly described as sheets of molecules parallel to the (a, b) planes, which stack along the c axis. However, the intermolecular interactions and their modification upon the change of spin are found to be very different. The intermolecular contacts can be classified into two kinds: those that occur within the (a, b) plane and those that involve molecular units belonging to different sheets. Within a sheet, the intermolecular interactions—contacts shorter than the sum of the van der Waals radii of two atoms—are mainly restricted to the interaction of the sulphur atom of the thiocyanate ligands with two carbon atoms of the bipy rings belonging to a consecutive $[Fe(bipy)_2(NCS)_2]$ molecule (see Fig. 5). The interatomic distances, S···C = 3.37, and 3.44 Å are well below what is expected for a normal S···C van der Waals distance, 3.70 Å, indicating the occurrence of strong intermolecular interactions. Six C···C π-interactions, ranging from 3.62 to 3.52 Å, are observed between the aromatic rings belonging to two molecules of consecutive sheets (van der Waals C···C distance ≈ 3.70 Å) (see Fig. 5 left). The inverse situation has been observed for the phen derivative, the π-interactions between $[Fe(phen)_2(NCS)_2]$ units are found within the (a, b) sheets and, more precisely, these interactions are

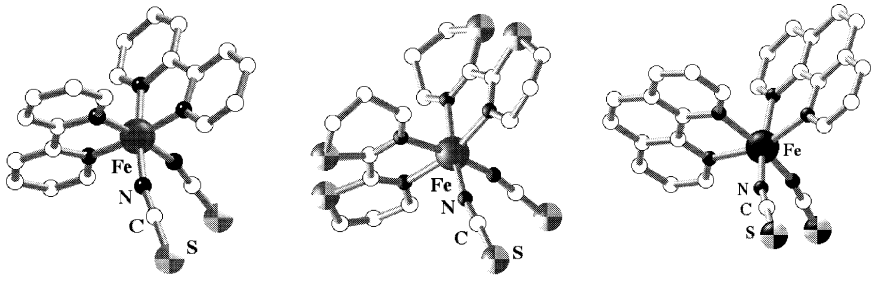

Fig. 2. Molecular structure of $[Fe(bipy)_2(NCS)_2]$, (left) $[Fe(btz)_2(NCS)_2]$ (centre), and $[Fe(phen)_2(NCS)_2]$ (left).

Table 1
Structural data of the $[Fe(L)_2(NCS)_2]$ family (L = bipy, phen, btz)

	$[Fe(bipy)_2(NCS)_2]$		$[Fe(phen)_2(NCS)_2]$			$[Fe(btz)_2(NCS)_2]$		
	298 K (10^3 HPa)	110 K (10^3 HPa)	293 K (10^3 HPa)	130 K (10^3 HPa)	1.0 GPa (293 K)	293 K (10^3 HPa)	130 K (10^3 HPa)	1.0 GPa (293 K)
a (Å)	13.2044(6)	12.9842(9)	13.161(2)	12.770(2)	12.656(3)	13.2880(11)	13.0551(17)	12.839(4)
b (Å)	10.1086(7)	9.8938(8)	10.163(1)	10.090(2)	9.848(2)	10.8610(11)	10.6504(17)	10.454(3)
c (Å)	16.4820(7)	16.1067(12)	17.480(2)	17.222(3)	16.597(4)	16.9199(19)	16.6717(39)	16.362(4)
V (Å^3)	2200.0(2)	2069.1(3)	2338()	2219()	2068.5()	2441.9	2318.1	2196.7
Fe–N(L) (Å)	2.173(4)	1.966(3)	2.206(3)	2.009(4)	1.989(9)	2.170(6)	1.973(7)	1.970(9)
Fe–NCS (Å)	2.053(5)	1.945(3)	2.057(4)	1.958(4)	1.954(7)	2.064(7)	1.948(8)	1.947(9)
ϕ°	14.7	7.7	13.7	8.0	4.7	12.0	8.3	4.5
Spin state	HS	LS	HS	LS	LS	HS	LS	LS

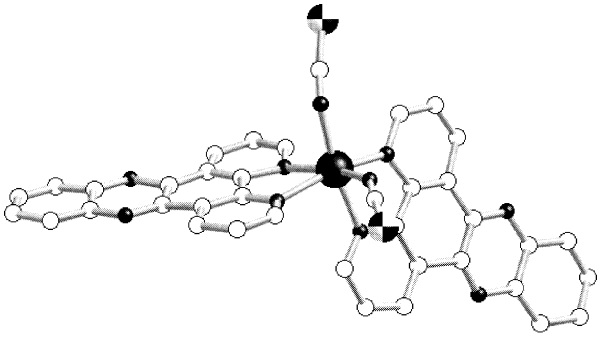

Fig. 3. Molecular structure of $[Fe(dpp)_2(NCS)_2]\cdot py$.

oriented in b direction. Each molecule defines ten short C···C contacts ranging from 3.4 to 3.52 Å with two adjacent molecules. Only one intermolecular contact occurs between two consecutive sheets (S···C ≈ 3.36 Å).

As far as the btz derivative is concerned, two weak intrasheet interactions at 3.684 and 3.646 Å are observed for the S···C and C···C contacts, respectively, and only one weak intersheet interaction has been observed between consecutive sheets, S···S = 3.685 Å.

The main feature of the crystal packing of $[Fe(dpp)_2(NCS)_2]$py arises from the extended aromatic nature of the ligand, which induces a large number of strong π interactions between dpp ligands of nearest $[Fe(dpp)_2(NCS)_2]$ units characterised by an interplanar distance between aromatic rings of 3.50 Å and a dihedral angle of 0.6° (Fig. 6).

It follows from this analysis that the key factor governing the cooperative nature of the spin change in the bipy, btz, phen and dpp derivatives is related to the number and strength of the intermolecular interactions directly associated to the aromatic or aliphatic nature of the ligands.

2.4. Thermal dilatation and compressibility studies on single crystals

The bond length shortening and bond angle variations, which are observed upon the change of spin state of the complex molecules, are transmitted to the whole crystal with different levels of efficiency depending on the effectiveness of the intermolecular interactions. These structural modifications induce lattice parameter variations that contain information about intensity and directionality of the intermolecular interactions. This information can be inferred from thermal dilation and high-pressure studies of a single crystal. Until now, these complementary studies have been carried out only for the phen and btz derivatives [12–27].

2.4.1. Thermal dilation data

Fig. 7 gives the evolution of the lattice parameters a, b, and c for $[Fe(btz)_2(NCS)_2]$ and $[Fe(phen)_2(NCS)_2]$. Their behaviour is very different. $[Fe(btz)_2(NCS)_2]$ presents a gradual evolution of a, b, and c, with a change of derivative at $T_c \approx 215$ K, whereas $[Fe(phen)_2(NCS)_2]$ exhibits a different thermal evolution for the three parameters. The a parameter remains almost constant in the whole range of temperature except at the vicinity of $T_c = 176$ K where it exhibits a discontinuous variation, 80% of this variation, $\Delta a \approx 0.21$ Å takes place in the 4 K range. The amplitude of the overall b variation is much more limited. The temperature dependence of b is smooth and quasi-linear in the whole range of temperatures but provides evidence for a small abrupt lattice dilatation close to the T_c region. In contrast, the evolution of c shows a continuous conversion similar to that observed for the btz derivative. All these data allow the evaluation of the linear and volume thermal expansion at constant pressure, $\alpha_i = (1/i)(\partial i/\partial T)_P$, ($i = a$, b, c, and V) and their respective anisotropy ratios defined as $3\alpha_i/\Sigma\alpha_V$ at a given temperature (Table 2). These ratios indicate that,

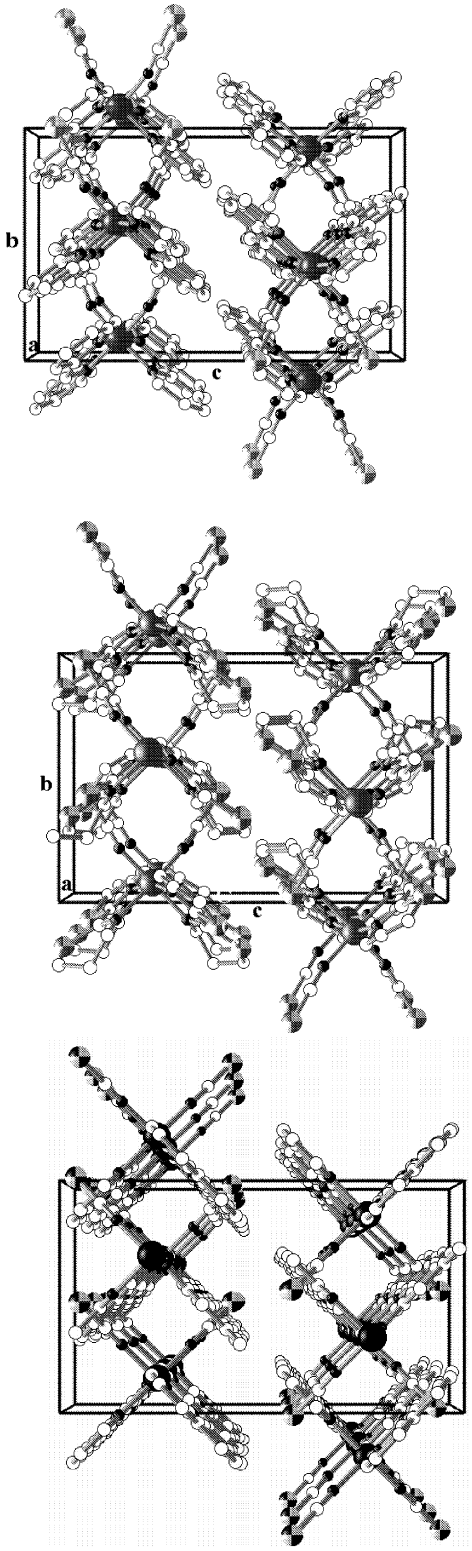

Fig. 4. Crystal packing of $[Fe(bipy)_2(NCS)_2]$ (top) and $[Fe(btz)_2(NCS)_2]$ (centre) and $[Fe(phen)_2(NCS)_2]$ (bottom).

for the btz derivative, there is no particular direction along which the structural arrangement is much more affected by temperature than in the other directions, in contrast, noticeable anisotropy is observed for the phen derivative.

Furthermore, a comparison between the thermal evolution of the unit cell volume and the $\chi_M T$ product clearly shows the following correlations between the magnetic and structural properties for these compounds (Fig. 7, bottom): (i) an abrupt change of the unit cell volume V is associated with the discontinuous spin transition of the phen derivative, whereas a continuous evolution of V is observed for the btz derivative, which exhibits a more gradual spin conversion, and (ii) the temperature at which the anomaly (discontinuity, or change of derivative sign) the temperature dependence of the lattice volume that occurs is in complete agreement with the spin transition temperature. However, this agreement between $\chi_M T$ and V versus T seems no longer valid as far as the $\chi_M T$ value remains constant (temperature range where there is no spin transition, see Fig. 7/bottom left). In such cases the evolution of V is only due to the thermal dilation (contraction) of the lattice, without any contribution resulting from the variation ΔR(Fe–N) of the metal-to-ligand bond distances and therefore from the modification of the $[FeN_6]$ core. The change of volume ΔV of the unit cell, 124 and 119 Å^3 for the btz and phen derivatives, respectively, can be separated into two contributions: the volume change ΔV_{SC} resulting from the spin crossover and the lattice thermal expansion ΔV_T [28]. ΔV_{SC}, and ΔV_T are 58 and 66 Å^3 for $[Fe(btz)_2(NCS)_2]$ and 60 and 59 Å^3 for $[Fe(phen)_2(NCS)_2]$, respectively. The V_{SC} values associated with the complete spin conversion can be estimated as 89 and 72 Å^3, which correspond to 22 and 18 Å^3 per formula unit, for $[Fe(btz)_2(NCS)_2]$ and $[Fe(phen)_2(NCS)_2]$, respectively.

2.4.2. Compressibility data

Fig. 8 displays the pressure dependence of the lattice parameters relative to their values at ambient temperature and pressure. The different behaviour of both derivatives is apparent from this figure. A significant change of derivative is clearly observed on a in $[Fe(phen)_2(NCS)_2]$, whereas a quasi-linear behaviour is observed for the same parameter in $[Fe(btz)_2(NCS)_2]$. Moreover, c decreases faster for the phen derivative, while b undergoes similar changes in both compounds [27]. The rapid evolution of a with pressure seems to be related to the spin change, as a similar effect has been observed in the dilatation experiments [12]. Long ago, Usha et al. studied the thermal dependence of the $\chi_M T$ at different pressures for the phen compound [29]. From these results it is possible to compare the pressure dependence of the molar fraction of HS molecules, n_{HS}, at room temperature with the pressure dependence of the relative change in the unit cell volume. Fig. 9 establishes a clear correlation between the cell volume change and the spin conversion. The characteristic

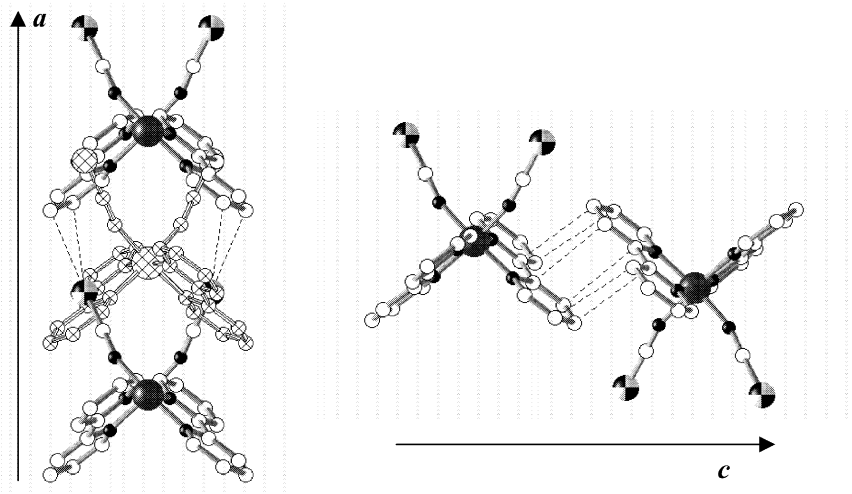

Fig. 5. Short intra-sheet S...C (left) and inter-sheet C...C (right) intermmolecular contacts in $[Fe(bipy)_2(NCS)_2]$.

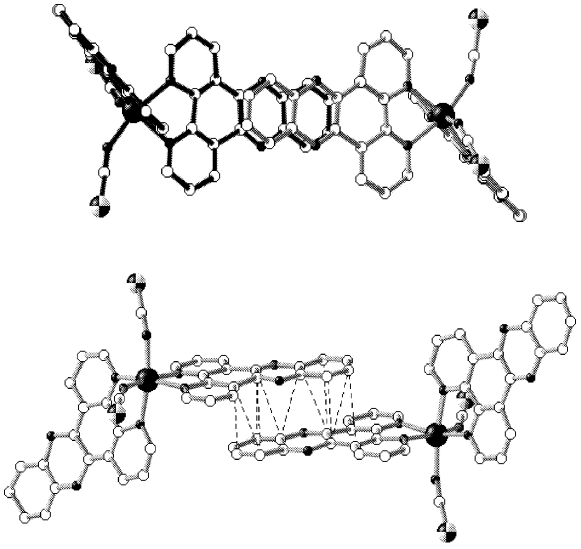

Fig. 6. Perspective view emphasising the π-stacking between two dpp ligands of consecutive $[Fe(bipy)_2(NCS)_2]$ units.

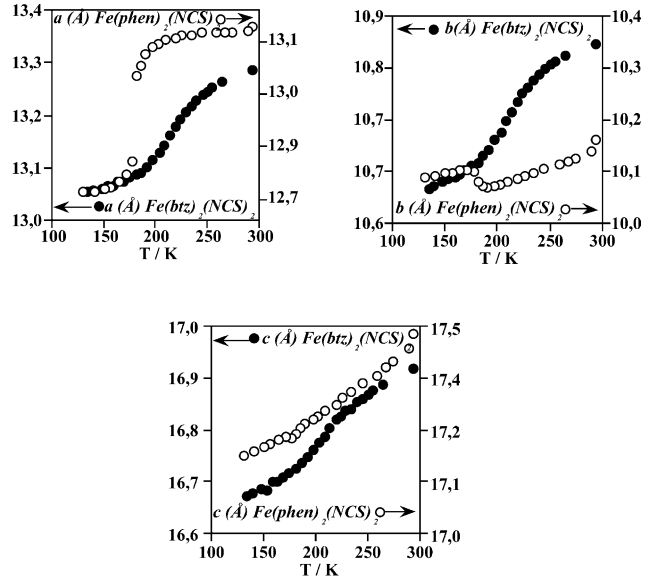

Fig. 7. Temperature dependence of the lattice parameters of phen (○) and btz (●) derivatives (top and middle). Comparison of $\chi_M T$ and V variations as a function of temperature for $[Fe(phen)_2(NCS)_2]$ (bottom, left) and $[Fe(btz)_2(NCS)_2]$ (bottom, right).

pressure, $P_{1/2}$, for $n_{HS} = n_{LS} = 0.5$ at room temperature, deduced from n_{HS} versus P plot and the maximun variation of (V/V_o) versus P are virtually equal to ca. 0.60 GPa. These results have been confirmed be EXAFS experiments, which yield a $P_{1/2} \approx 0.6$–0.7 GPa for $[Fe(phen)_2(NCS)_2]$ polymorph II [30]. Concerning $[Fe(btz)_2(NCS)_2]$, no drastic anomaly is observed in the whole range of pressures. Only a quasi-linear behaviour with a small change of slope is observed at $P \approx 0.4$ GPa.

The unit cell contraction at 1 GPa $\Delta V = 269$ and 251 $Å^3$ for $[Fe(phen)_2(NCS)_2]$ and $[Fe(btz)_2(NCS)_2]$, respectively, is about twice as much as those observed in thermal expansion experiments. Following the method proposed by Wiehl et al. [28], it is possible to estimate the variation in the unit cell volume due only to the spin crossover, $(\Delta V_{SC})_P = 72$ $Å^3$, which is in perfect agreement with the value obtained from dilation measurements $(\Delta V_{SC})_T$. For $[Fe(btz)_2(NCS)_2]$ no thermal variation of the magnetic properties under pressure data are available and, consequently, this makes a confident estimate of $(\Delta V_{SC})_P$ impossible.

Table 2
Thermal expansion and compressibility data of $[Fe(phen)_2(NCS)_2]$ and $[Fe(btz)_2(NCS)_2]$

	$[Fe(phen)_2(NCS)_2]$		$[Fe(btz)_2(NCS)_2]$	
Expansion data				
T (K)	293	130	293	130
$\alpha_a/10^{-4}$ K^{-1}	0.22	0.72	0.80	0.47
$\alpha_b/10^{-4}$ K^{-1}	0.83	0.45	0.74	0.65
$\alpha_c/10^{-4}$ K^{-1}	1.15	0.70	0.72	0.58
$\alpha_v/10^{-4}$ K^{-1}	1.20	1.87	2.26	1.70
$3\alpha_i/\alpha_v$	0.3:1.1:1.6	1.2:0.7:1.1	1.1:1.0:1.0	0.8:1.1:1.0
ΔV/Å^3	119		124	
ΔV_T/Å^3	59		66	
ΔV_{SC}/Å^3	60 (72)		58 (89)	
Compressibility data				
P	10^3 HPa	1.0 GPa	10^3 HPa	1.0 GPa
$k_a/10^{-2}$ GPa^{-1}	2.1	1.6	4.1	2.8
$k_b/10^{-2}$ GPa^{-1}	3.3	2.8	4.3	3.3
$k_c/10^{-2}$ GPa^{-1}	5.3	7.0	3.7	2.8
$k_v/10^{-2}$ GPa^{-1}	10.7	8.2	12.1	8.9
$3k_i/k_v$	0.6:0.9:1.5	0.6:1.0:1.4	1.0:1.1:0.9	0.9:1.1:0.9
ΔV/Å^3	269		251	
ΔV_{SC}/Å^3	60 (72)		–	

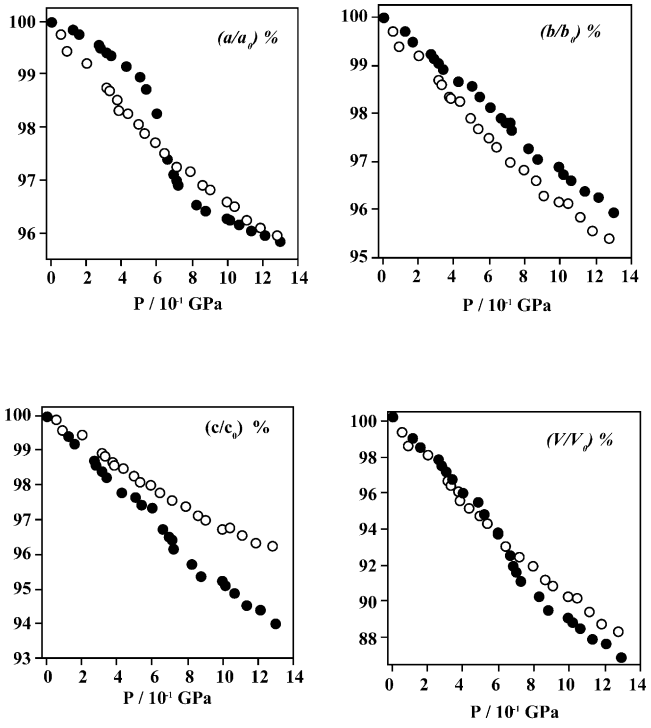

Fig. 8. Evolution of the lattice parameters, as fractions of ambient pressure-room temperature values, at variable pressure: (●) $[Fe(phen)_2(NCS)_2]$, (○) $[Fe(btz)_2(NCS)_2]$.

The values of linear (k_i) and volume (k_V) compressibility coefficients deduced from the pressure dependence of the lattice parameters, as well as the corresponding anisotropies, have been deduced and gathered in Table 2. Again, a significant anisotropy is observed in the linear coefficients of $[Fe(phen)_2(NCS)_2]$, whereas $[Fe(btz)_2(NCS)_2]$ exhibits an almost isotropic compressibility. The anisotropy of $[Fe(phen)_2(NCS)_2]$ is slightly reduced at high pressure, however, a remains the stiffest direction while c the most compressible. Both complexes exhibit very close values of volume compressibility at low and high pressure, nevertheless, $[Fe(phen)_2(NCS)_2]$ is a little stiffer than $[Fe(btz)_2(NCS)_2]$. These results are in close agreement with the Spiering's model based on the elasticity theory, in which the sharpness of the temperature-driven spin transition depends on the stiffness of the crystal lattice [31].

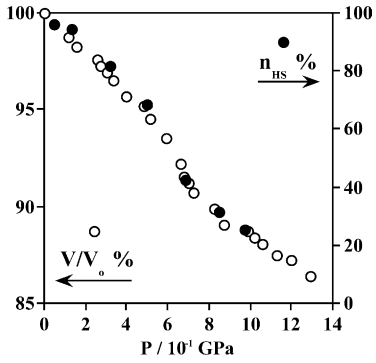

Fig. 9. Pressure dependence of the unit-cell volume (○) (as fraction of ambient pressure-room-temperature value) and of the HS fraction n_{HS}(%)(●) (deduced from Usha et al data [29]) for $[Fe(phen)_2(NCS)_2]$.

2.5. Concluding remarks

From variable temperature and pressure X-ray single crystal studies, it has been inferred that the intramolecular changes upon spin conversion do not play a key role in determining the different cooperative character of the transition as a similar molecule volume change has been deduced for $[Fe(btz)_2(NCS)_2]$ and $[Fe(phen)_2(NCS)_2]$.

Dilatation and compressibility experiments have demonstrated that the main difference between phen and btz derivatives arises from the anisotropy observed in the linear dilatation and compressibility coefficients. Qualitatively, a certain correlation between such a lattice anisotropy and the spatial distribution of intermolecular contacts has also been observed. In the case of $[Fe(phen)_2(NCS)_2]$, the lowest values of the dilatation linear coefficient concern the axes a and b, which define the above-mentioned sheets where molecules are stacked. It is worth mentioning that the small variation in b's direction upon cooling down, characterised by a small dilatation at temperatures close to T_c, is due to the π-stacking between consecutive phen ligands, which takes place only in this direction. Similarly, the lowest values of linear compressibility, associated to the stiffest lattice directions, also concern the axes a and b. On the other hand, c direction shows the greatest dilatation and

compressibility coefficients as it corresponds to the intersheet direction for which far fewer contacts are observed. The lack of significant intermolecular interactions induces an isotropic distribution of weak intermolecular contacts in $[Fe(btz)_2(NCS)_2]$.

To conclude, we have observed that by playing with the nature of the ligands, aliphatic, aromatic, or extended aromatic, it is possible to create stronger cohesive forces and receive a more cooperative signal from the compound.

3. 2,2′-Bipyrimidine bridged iron(II) dinuclear spin crossover complexes

The design and synthesis of polynuclear spin crossover compounds represents an alternative strategy to explore cooperativity. Moreover, new kinds of spin crossover regimes related with nuclearity of the system may be observed. Tightly related to this strategy is the idea of combining two different electronic properties like magnetic exchange and spin crossover in the same molecule, which was realised by Kahn and developed together with Real et al. in the second half of the 1980s. This work is based on 2,2′-bipyrimidine bridged iron(II) compounds.

2,2′-Bipyrimidine (bpym) is a bis(α-diimine) ligand whose similarity with the well known bipy and phen ligands has attracted the attention of chemists in the last 20 years. Like bipy and phen, bpym is a middle-strong field ligand which can induce spin crossover behaviour in iron(II) complexes in the appropriate coordination surroundings. The most significant difference between bpym and bipy or phen is that the former can act as a bis-chelating ligand and mediate electronic effects between metal centres in the resulting polymetallic species [32–38].

The dinuclear compound $\{[Fe(H_2O)_4]_2bpym\}(SO_4)_2$ can be considered as a precursor of more elaborate bpym based magnetic systems [39]. In this centrosymmetric molecule, the iron atom is coordinated to four water molecules and to two nitrogen atoms of the bpym

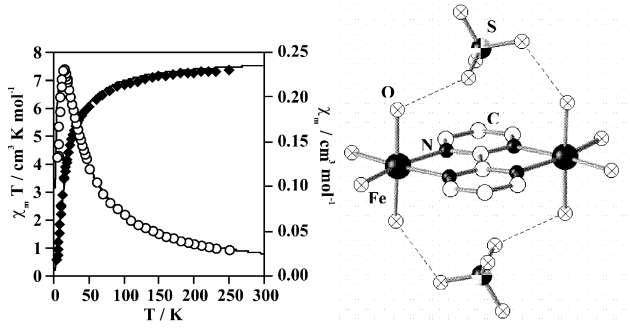

Fig. 10. Magnetic behaviour [χ_M T(●); χ_M(○)] (left), and molecular structure of $\{Fe(H_2O)_4]_2bpym\}(SO_4)_2$ (right).

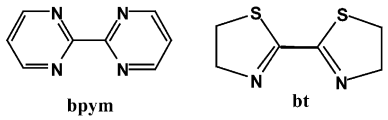

Scheme 2.

ligand. Each apical water molecule is hydrogen bonded to one sulphate counterion (Fig. 10). The iron(II) atom is in the HS state and interacts antiferromagnetically through bpym ($J = -3.4$ cm^{-1}). The formal substitution of the water molecules by more appropriate ligands like bpym, 2,2′-bithiazoline (bt), 6-methylbipy or 2,2′-dipyridylamine together with NCS^- or $NCSe^-$ counter-ions affords a family of binuclear compounds which displays a rich variety of magnetic behaviour (Scheme 2).

In this section our attention will focus on the following four members of the bpym-bridged iron(II) family of complexes: $\{[Fe(L)(NCX)_2]_2bpym\}$ (L = bpym, bt; X = S, Se) (hereafter noted (**L**, **X**)).

3.1. Structural characterisation

The centrosymmetric dinuclear units $\{[Fe(L)(NCS)_2\}]_2bpym\}$, where L = bpym [40] or bt [41], are shown in Fig. 11. Each iron(II) atom is surrounded by two NCS^- anions in the *cis* position, two nitrogen atoms of the bridging bpym ligand and the remainder positions are occupied by the peripheral bpym or bt ligands. The $[FeN_6]$ chromophore is rather distorted with Fe–N bond distances characteristic for an iron(II) ion in the HS state (see Table 3).

No thermal spin transition is observed for (**bpym**, **S**) in the whole range of temperature (see Section 3.2). At first sight this is a rather unexpected result, as the iron(II) environment in the dinuclear compound is close to that of the $[Fe(bipy)_2(NCS)_2]$. However, the average Fe–N bond distance is noticeably greater for (**bpym**, **S**). In contrast, the derivative (**bt**, **S**), which shows shorter Fe–N bond distances than (**bpym**, **S**), undergoes a complete spin transition [42]. The remaining members of this family, (**bpym**, **Se**) and (**bt**, **Se**) [43], also undergo spin transition but their crystal structures have not been studied yet. However, structural information on these compounds has been obtained using X-ray absorption techniques (EXAFS) at 300 and 77 K. The EXAFS data afforded a rather satisfactory description of the iron(II) coordination core both in the HS and in the LS state for these compounds [43].

3.2. Magnetic properties

The magnetic behaviour of this series is depicted in Fig. 12. As stated before, (**bpym**, **S**) does not display thermal induced spin conversion but intramolecular

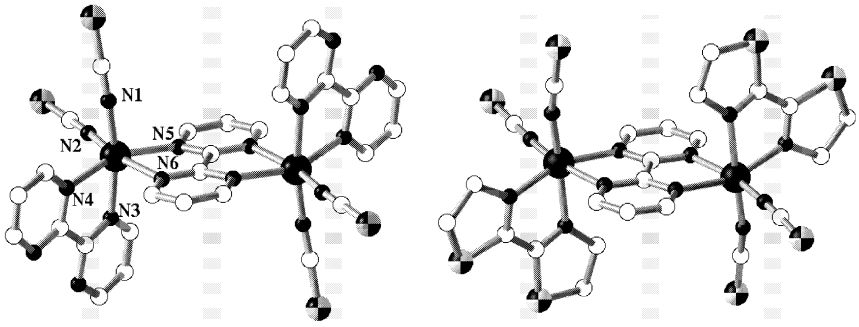

Fig. 11. Molecuar structure of {[Fe(bpym)$(NCS)_2$}]$_2$bpym} (left), and {[Fe(bt)$(NCS)_2$}]$_2$bpym} (right).

Table 3
Fe–N bond distances for the binuclear compounds (**bpm**, **S**) and (**bt**, **S**)

Bond length (Å)	(**bpym**, **S**)	(**bt**, **S**)
Fe–N1	2.078(6)	2.069(14)
Fe–N2	2.051(7)	2.041(13)
Fe–N3	2.200(6)	2.239(12)
Fe–N4	2.211(6)	2.112(12)
Fe–N5	2.316(6)	2.195(13)
Fe–N6	2.223(6)	2.256(11)

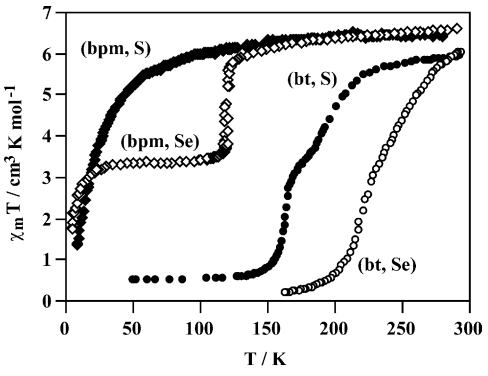

Fig. 12. Magnetic properties of the family {[Fe(L)$(NCS)_2$}]$_2$bpym}.

antiferromagnetic coupling between the two iron(II) ions through the bpym bridge ($J = -4.1$ cm^{-1}, $g = 2.18$) is observed. When thiocyanate is replaced by selenocyanate the resulting (**bpym**, **Se**) derivative shows an abrupt spin transition in the 125–115 K temperature region with a small hysteresis loop ca. 2.5 K wide. Only 50% of the iron(II) atoms undergo spin transition. The decrease of the $\chi_M T$ versus T curve at lower temperatures is due to the occurrence of local zero-field splitting of the $S = 2$ state (see below). The magnetic properties of (**bt**, **S**) and (**bt**, **Se**) are similar and show a complete spin transition with the remarkable singularity of taking place in two steps centred at 163 and 197 K for (**bt**, **S**) and at 223 and 265 K for (**bt**, **Se**). In both cases, the plateau corresponds approximately to 50% of spin conversion.

These macroscopic steps, also detected by means of Mössbauer spectroscopy and calorimetric measurements, were interpreted in terms of a microscopic two-step transition between the three possible spin pairs of each individual molecule [43]:

[LS–LS]↔[LS–HS]↔[HS–HS]

The stabilisation of the [LS–HS] mixed-spin pair was associated to the synergistic effect between intramolecular and cooperative intermolecular interactions.

The common peculiarity of the spin crossover process in all dinuclear compounds studied so far, is the plateau in the spin transition curve. The natural explanation of this fact is that one half of the initial iron(II) atoms in the HS state has converted to the LS state. Two possible channels of HS–HS pairs transformation at decreasing temperature may be proposed: [HS–HS]↔[LS–HS] or [HS–HS]↔[LS–LS]. The conjecture of the existence of the [LS–LS], [LS–HS], and [HS–HS] spin pairs has recently been solved in terms of direct physical measurements, which confirm they really exist. One, macroscopic, is based on magnetisation versus magnetic field measurements [44], and the other one, microscopic, based on the Mössbauer spectroscopy carried out in an externally applied magnetic field [45].

3.3. Influence of pressure dependence on the thermal variation of the magnetic susceptibility

The pressure dependence of the thermal variation of $\chi_M T$ represents a good probe to show that the occurrence of the singular [LS–HS] spin pairs is not fortuitous but a reliable species consubstantial with the dinuclear nature of the complexes [44].

It has already been shown that hydrostatic pressure favours the LS state in mononuclear complexes, and there is no reason to think it should be otherwise for dinuclear species. Two members of the {[Fe(L)-$(NCS)_2$]$_2$bpym} family are particularly good candidates in this regard: (**bpym**, **S**) and (**bpym**, **Se**). Fig. 13 displays the thermal dependence of $\chi_M T$ at different pressures.

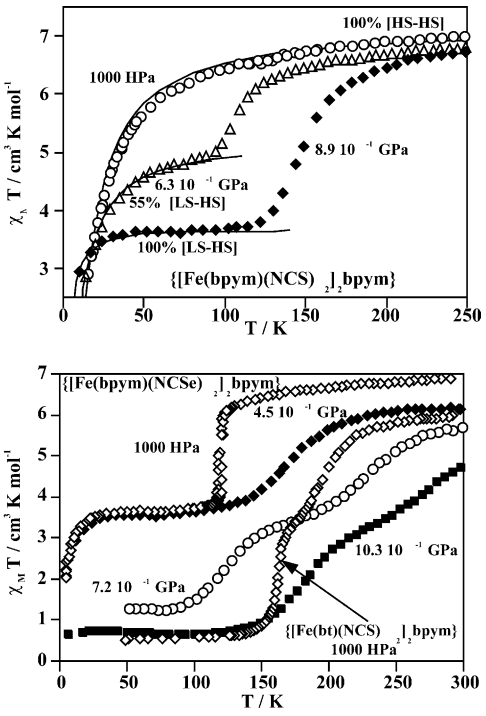

Fig. 13. Temperature dependence of $\chi_M T$ at different pressures for (**bpym, S**) (top) and (**bpym, Se**) (bottom). The solid lines, together with estimated percentages of [LS-HS] and [HS-HS] species, correspond to the calculations using the Hamilltonians $\boldsymbol{H} = -J\boldsymbol{S}_a\boldsymbol{S}_b + \boldsymbol{S}_a D_a \boldsymbol{S}_a + \boldsymbol{S}_b D_b \boldsymbol{S}_b + \beta(S_a g_a + \boldsymbol{S}_b g_h)\ H$ and $\boldsymbol{H} = D[S_z^2 - (1/3)\ S(S+1)] + g\beta HS$. The two-step transition of (**bt, S**) at ambient pressure has been included for comparison.

At ambient pressure, and in the whole range of temperatures, (**bpym**, **S**) is constituted only by the antiferromagnetically coupled [HS–HS] pairs. When pressure increases up to 6.3×10^{-1} GPa a partial conversion from 100% [HS–HS] to 55% [LS–HS] species takes place, and finally for $P = 8.9 \times 10^{-1}$ GPa the total conversion to [LS–HS] spin pair is accomplished. It is worth noting that, at this pressure, (**bpym**, **S**) undergoes a similar [HS–HS]↔[LS–HS] spin transition at $T_c \approx 150$ K like that of (**bpym**, **Se**) at ambient pressure. The effect of pressure on the thermal dependence of (**bpym**, **Se**) induces a loss of cooperativity and a shift of T_c towards higher temperatures for pressures lower than 4.5×10^{-1} GPa. For higher pressures, a second transition appears in addition to the former; between 7.2 and 10.3×10^{-1} GPa a two-step transition is observed (see Fig. 13).

As mentioned above, the common peculiarity of the spin crossover process in all dinuclear compounds studied so far is a plateau in the spin transition curve. From the analysis of pressure experiments, it follows that its nature is determined by the formation of [LS–HS] pairs and intermolecular interactions, which provide the stability of crystal domains with [LS–HS] pairs. Indeed, in the absence of intermolecular interactions, the increase of pressure should decrease the amount of HS fraction. The pressure induced low-temperature state of (**bpym**, **S**) consisting almost entirely of the [LS–HS] units is stable at least up to 11×10^{-1} GPa. For (**bpym**, **Se**), a pressure of 4.5×10^{-1} GPa shifts T_c by ca. 50 K upward without increasing the amount of LS fraction. Only at higher pressures the second step appears for this derivative. These experimental data underline the role of long-range interactions in the stabilisation of the hypothetical "chess board"-like structure consisting of [LS–HS] units.

3.4. Photo-switching between spin pairs

In 1984, Decurtins et al. discovered that by light irradiation with green light, the compound $[Fe(ptz)_6](BF_4)_2$ (ptz = 1-propytetrazole) at 20 K could be converted from the stable LS state to the metastable HS state [46]. Later, Hauser reported the reverse-LIESST effect, wherein red light is used to convert the compound back into the LS state [47].

Up to now, most of the spin crossover compounds exhibiting LIESST properties are assemblies of monomeric units with through-space rather than through bond interactions. In this section, we will report a new aspect of the photomagnetism of spin crossover iron(II) compounds occurring in polynuclear species.

A few years ago a form of synergy was pointed out between magnetic interaction and spin conversion in the presence of light in the (**bpym**, **Se**) and (**bt**, **S**) systems [45,48,49]. In these compounds the corresponding ground states [LS–HS] and [LS–LS] were converted, partially, to the metastable [HS–HS] spin pair state after irradiation with visible light ($\lambda = 647$–676 nm). Consequently, the magnetic properties of the former complexes after LIESST effect were found very close to those of (**bpym**, **S**). This is not an unexpected result taking into account that the bridge in (**bpym**, **Se**) and (**bt**, **S**) is strictly the same as that of (**bpym**, **S**) and that the interaction parameter, J, in a coupled binuclear compound depends essentially on the nature of the bridging ligand. In contrast, for mononuclear spin crossover system it has been reported that the HS molar fraction after irradiation remains nearly constant in the tunnelling region where the kinetics of the relaxation back to the LS state are very slow [4].

4. Polymeric spin crossover compounds

4.1. One-dimensional coordination polymers

Self-assembly of molecules driven by coordination to transition metal ions has motivated intense research activity because of their chemical and structural diversity, potential functionality and beauty. Self-assembly also represents an important tool to systematically

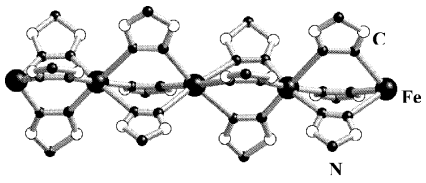

Fig. 14. Structure of the polymeric $[Fe(triazole)_3]^{2+}_n$ spin crossover cation deduced from EXAFS data [58].

explore cooperativity as the coordination geometry of iron(II) and its modification upon spin conversion may be propagated into infinite architectures of varying dimensionality and topology. The first one-dimensional (1D) polymeric spin crossover compound corresponds to the $[Fe^{II}(4\text{-R-trz})_3](anion)_2\ xH_2O$ (4-R-trz = 4-substituted 1,2,4-triazole) family, which was reported by Lavrenova et al. and reinvestigated by Kahn and coworkers [50–57]. In this system the iron atom is triple-bridged by triazole ligands through the nitrogen atoms occupying the 1- and 2-positions and defining a linear chain [58] (Fig. 14).

The nature of the spin conversion depends on the substituent in position 4, the counterion and the non-coordinating molecules of solvent. Some compounds in this series show very abrupt spin transitions with a thermal hysteresis width of up to 35 K. In contrast, the 1D spin crossover compound $[Fe(btzp)_3](ClO_4)_2$ (btzp = 1,2-bis(tetrazol-1-yl)propane) recently reported undergoes a continuous spin conversion [59]. The rigidity of the triazole iron bridged chain and the flexibility of the unsaturated linkages connecting the two tetrazole rings seems to be the reason for the different cooperativity observed in these 1D compounds (Scheme 3).

Despite these examples, the number of polymeric 1D spin crossover compounds reported up to now is still scarce. In this respect, we have paid attention to the bifunctional chelating bidentate ligand bpym and the bismonodentate rod-like ligands of the polypyridine type like 4,4′-bipyridine (4,4′-bipy) because they have proved to be particularly suitable both for metallo-supramolecular chemistry as well as for the field of spin crossover phenomenon (Scheme 4).

The structure of this complex is made up by neutral chains formed by $Fe(NCS)_2$ units, bridged by bis-bidentate bpym molecules [60]. A perspective drawing of a chain is depicted in Fig. 15. Because the 4_1 screw axis along the z-axis, the chains assume a right-handed

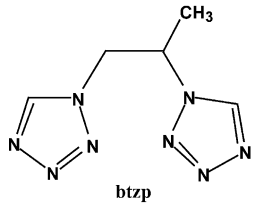

Scheme 3.

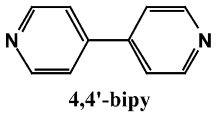

Scheme 4.

(Δ) homochiral conformation. Each iron atom is in a distorted $[FeN_6]$ octahedral environment defined by the nitrogen atoms belonging to two thiocyanate ligands in *cis* position and to two bipym ligands. The Fe–N bond distances involving the thiocyanate ligands, [Fe–N5 = 2.028(4) Å and Fe–N6 = 2.084(3)Å], are much shorter than those concerning the bpym ligands, [Fe–N1 = 2.218(4) Å, Fe–N2 = 2.265(3) Å, Fe–N3 = 2.260(4) Å, and Fe–N1 = 2.220(4) Å]. As far as the iron environment is concerned, the structure of this compound is similar to that of the binuclear compound (**bpym**, **S**). The main differences between the two compounds are: (i) (**bpym**, **S**) contains terminal and bridging bpym groups whereas in [Fe(2,2′-bpym)$(NCS)_2$] bpym acts as a bridging ligand, and (ii) the relative displacement of adjacent iron atoms. In (**bpym**, **S**), both thiocyanate groups bonded to the first atom are in an opposite position (*anti*) with respect to those bonded to the second due to an inversion centre, which is placed in the middle of the bpym molecule. However, in the chain compound the presence of a C_4 axis allows the *syn* disposition of two thiocyanate groups bonded to two adjacent iron atoms while the other two are in *anti*.

The magnetic behaviour shows that at ambient pressure this complex is HS in the whole range of temperature. As in the (**bpym**, **S**) derivative the magnetic behaviour is dominated by intramolecular magnetic exchange mediated by the bpym bridge, which extends along the 1D system [60]. However, [Fe(2,2′-bpym)$(NCS)_2$] undergoes thermal spin transition at pressures noticeably much higher than (**bpym**, **S**) [44]. The curve measured at 0.98 GPa shows no indication of spin crossover; at 1.18 GPa, however, there is a half spin transition between 100 and 150 K (Fig. 16). The significantly higher pressures required to trigger the spin transition in [Fe(2,2′-bpym)$(NCS)_2$] with respect to (**bpym**, **S**) are rather surprising in view of their molecular structures. The average Fe–N bond distances can be considered the same in both compounds (2.180 and 2.179 Å for (**bpym**, **S**) and [Fe(2,2′-bpym)$(NCS)_2$], respectively), and consequently, the ligand field strength is expected to be very similar in both compounds. So, the difference in sensitivity to pressure induced spin conversion should be attributed to the different packing of active centres in the crystal lattice.

It is well known that ligands like 1,2-di-(4-pyridyl)-ethylene, 1,4-bis-(4-pyridyl)-butadyine or 4,4′-bis-1,2,4-triazole represent good examples of rod-like bifunctional ligands suited to the synthesis of spin-crossover

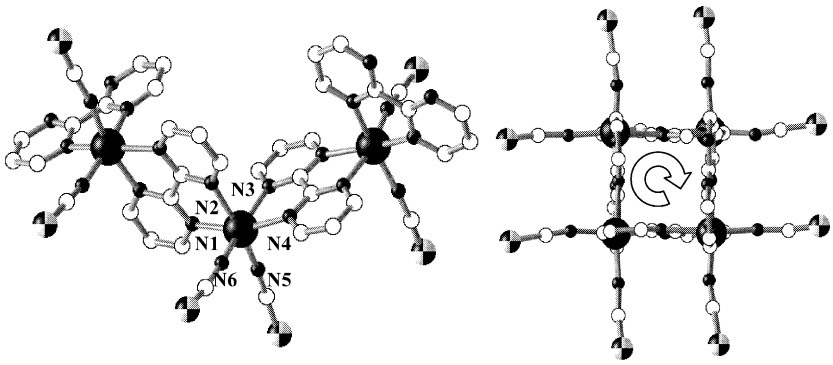

Fig. 15. Perpendicular (left) and parallel (right) views to the four-fold screw axis characteristic of the $[Fe(2.2'\text{-bpym})(NCS)_2]_n$ homo-chiral chain.

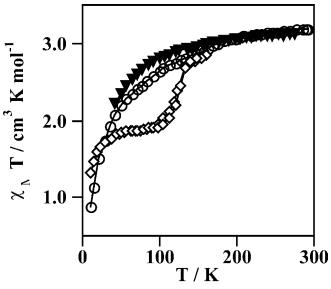

Fig. 16. Temperature dependence of $\chi_M T$ for $[Fe(2.2'\text{-bpym})(NCS)_2]_n$ at different pressures: 1000 Hpa (▼), 0.98 GPa (○), and 1.18 GPa (◇).

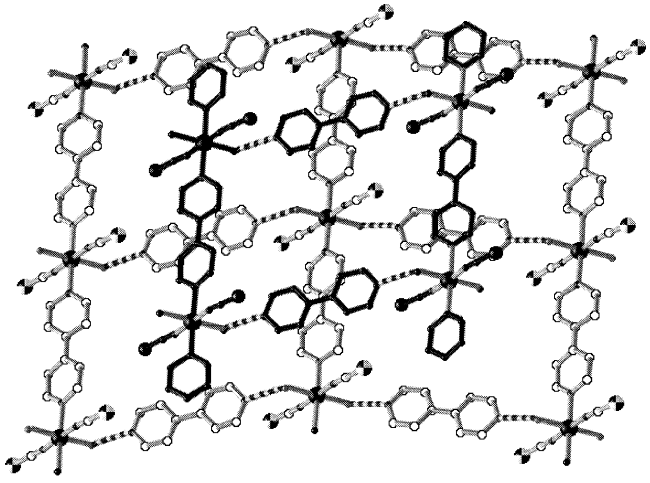

Fig. 17. Molecular structure of $[Fe(4,4'\text{-bipy})(H_2O)_2(NCX)_2]\cdot 4,4'$bipy with X = S or Se.

coordination polymers. When these ligands react with [iron(II)/2 NCS^-] solutions, the solvent molecules of the first coordination sphere of the metal ion are usually replaced to give square-grid motives (see Section 4.2). However, extrapolation of these results to the ligand L = 4,4′-bipy is no longer valid due to the formation of very effective hydrogen bonds between uncoordinated ligands and coordinated solvent molecules. This fact prevents further substitution of solvent molecules by the 4,4′-bipy ligand giving very stable $[Fe(4,4'\text{-bipy})(H_2O)_2(NCX)_2]\cdot 4,4'$-bipy (X = S [61,62], Se [61]) linear chains. In spite of this, the crystal structure of $[Co(4,4'\text{-bipy})_2(NCS)_2]$ $2(CH_3CH_2)_2O$ has been reported [63]. However, in water or methanol solutions the stable species are $[Fe(4,4'\text{-bipy})(H_2O)_2(NCX)_2]\cdot 4,4'$-bipy (X = S, Se). In the solid state, these systems are made up of linear chains running in a parallel direction. These chains consist of $[Fe(solvent)_2(NCS)_2]$ planar units bridged by L. A second type of L ligand intercalated between the chains is hydrogen-bonded defining a second system of zig-zag chains perpendicular to the linear system of chains. Hence, the uncoordinated ligands connect adjacent linear chains defining corrugated layers. The layers alternate in such a way that the iron atom, in an adjacent layer, is above and below the centre of the rectangles defined by the two systems of chains (Fig. 17).

Due to their reliability and solubility in water–methanol, these compounds may be considered precursors of new polymeric iron(II) spin crossover complexes. So, substitution of the solvent molecules in $[Fe(4,4'\text{-bipy})(H_2O)_2(NCX)_2]\cdot 4,4'$-bipy (X = S, Se) by more appropriate N-donor ligands like bt affords new 1D spin crossover polymeric compounds of the type $[Fe(4,4'\text{-bipy})(bt)(NCX)_2]$ [64]. The S and Se derivatives are iso-structural; the structure for X = S is depicted in Fig. 18. This compound consists of parallel linear chains defined by *trans*-4,4′-bipy linked to iron(II) ions. The equatorial plane is defined by two nitrogen atoms of one bt ligand and two thiocyanate groups in *cis* position. The coordination octahedron of iron(II) is strongly distorted.

The magnetic behaviour of these derivatives shows that a very incomplete spin transition occurs. The incomplete character of the transition is a consequence of the low temperatures at which the conversion takes place. For temperatures lower than ca. 70 K the kinetics of the HS-to-LS process becomes slow enough to quench the spin transition (Fig. 19).

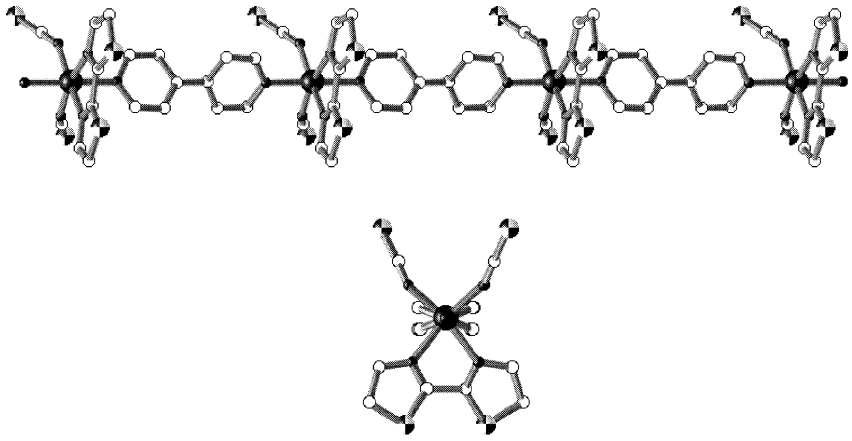

Fig. 18. Perpendicular (top) and parallel (bottom) views of the chain $[Fe(4,4'\text{-bipy})(bt)(NCX)_2]$ with X = S or Se.

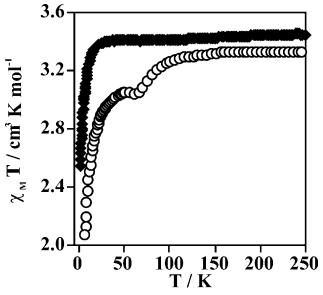

Fig. 19. Magnetic properties of the high spin $[Fe(4,4'\text{-bipy})(H_2O)_2(NCS)_2]\cdot 4,4'\text{-bipy}$ (◆) and $[Fe(4,4'\text{-bipy})(bt)(NCX)_2]$ (○) species.

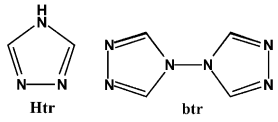

Scheme 5.

4.2. Two-dimensional coordination polymers

There is a relatively small number of two-dimensional (2D) spin crossover compounds and most of them belong to the $[FeL_2(NCS)_2]$ *n*S series where L is a bis-monodentate ligand. Two relevant members of this family were derived by Engelfriet and Haasnoot from L = 1,2,4-triazole (Htr) and 4,4′-bitriazole (btr) [65] (Scheme 5). The N2,N4 and N1,N1′ bridging modes of the Htr and btr ligands lead to 2D layered compounds of composition $[Fe(Htr)_2(NCS)_2]$ [66] and $[Fe(btr)_2(NCS)_2]\ H_2O$ [67], respectively (see Fig. 20). In these systems, the iron(II) ions are surrounded by four nitrogen atoms belonging to the triazole rings and two thiocyanate anions fill the apical positions of the compressed octahedron. The Htr or btr ligands bridge two iron atoms defining an infinite stack of layered grids. Both compounds exhibit interesting but different

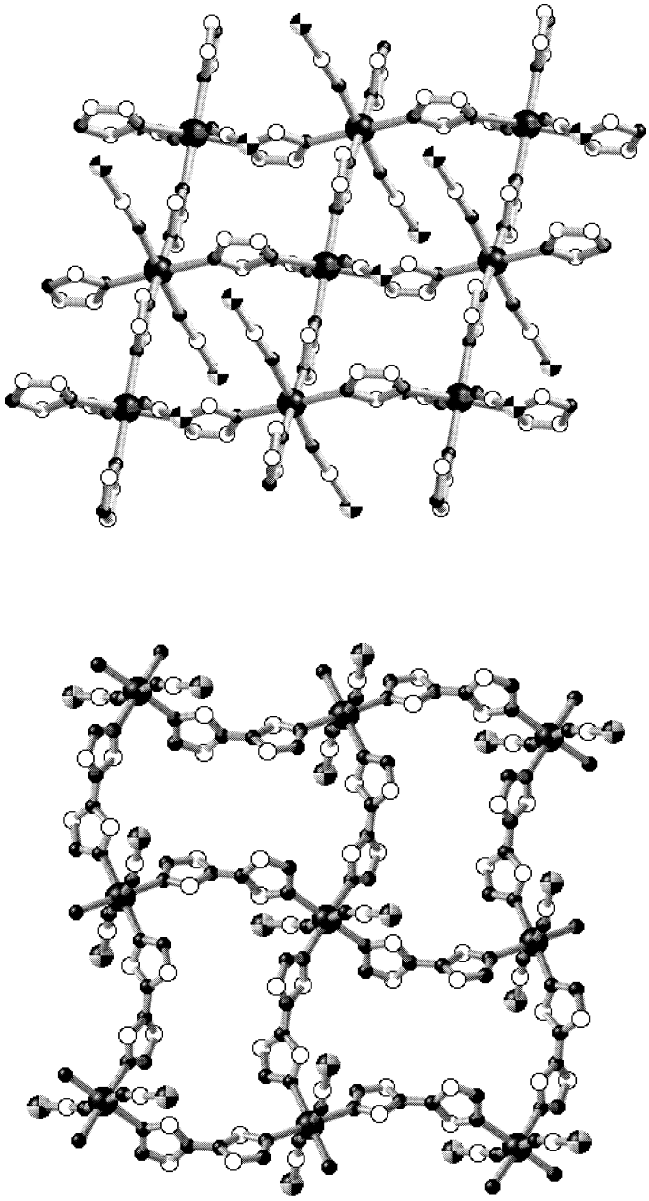

Fig. 20. Molecuar structure of $[Fe(Htr)_2(NCS)_2]$ (top) and $[Fe(btr)_2(NCS)_2]\cdot H_2O$ (bottom).

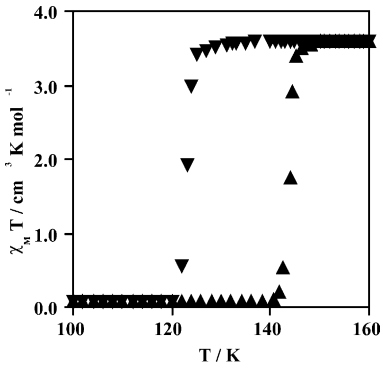

Fig. 21. Magnetic behaviour of $[Fe(btr)_2(NCS)_2]\cdot H_2O$.

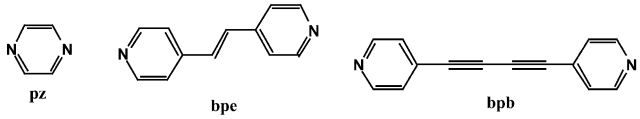

Scheme 6.

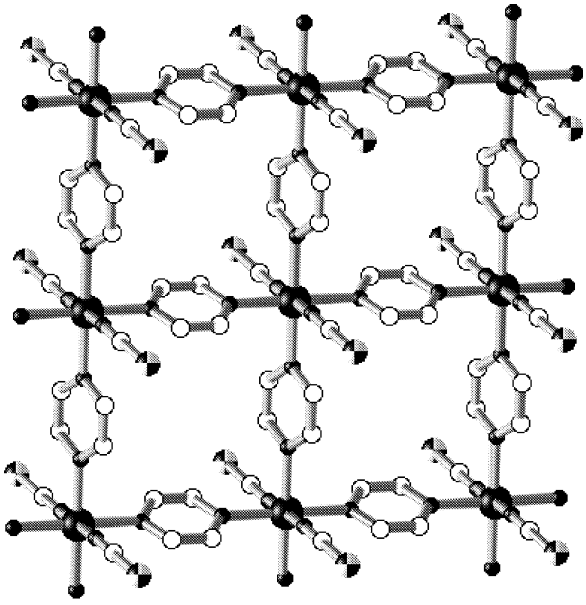

Fig. 22. Molecuar structure of $[Fe(pz)_2(NCS)_2]$.

magnetic behaviour. The former does not undergo spin transition as the iron(II) atoms are in the HS state irrespective of temperature. However, the ligand Htr allows magnetic exchange affording a 2D-Ising system [68]. The field strength induced by the ligand btr around the iron(II) ion is stronger than that of Htr as to induce a cooperative spin transition centred at 130 K with 20 K of hysteresis width [69] (Fig. 21). This compound represents the first fully characterised 2D spin crossover system and has been subject to intense research in order to investigate its cooperative nature, for instance, dilution [70], as well as hydrostatic pressure effects on the thermal induced spin transition behaviours [71,72].

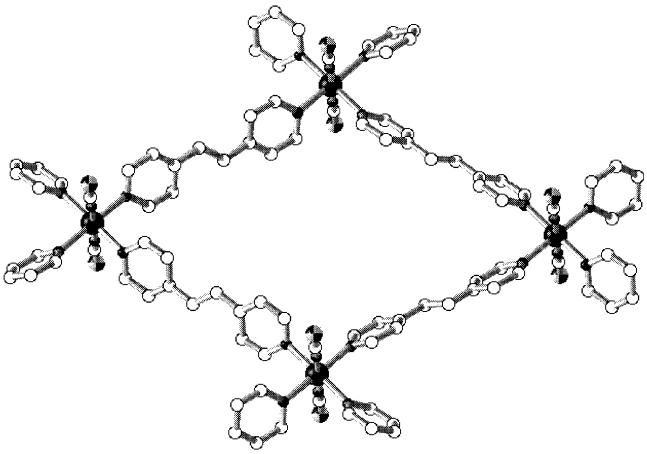

Fig. 23. Molecuar structure of $[Fe(bpe)_2(NCS)_2]CH_3OH$.

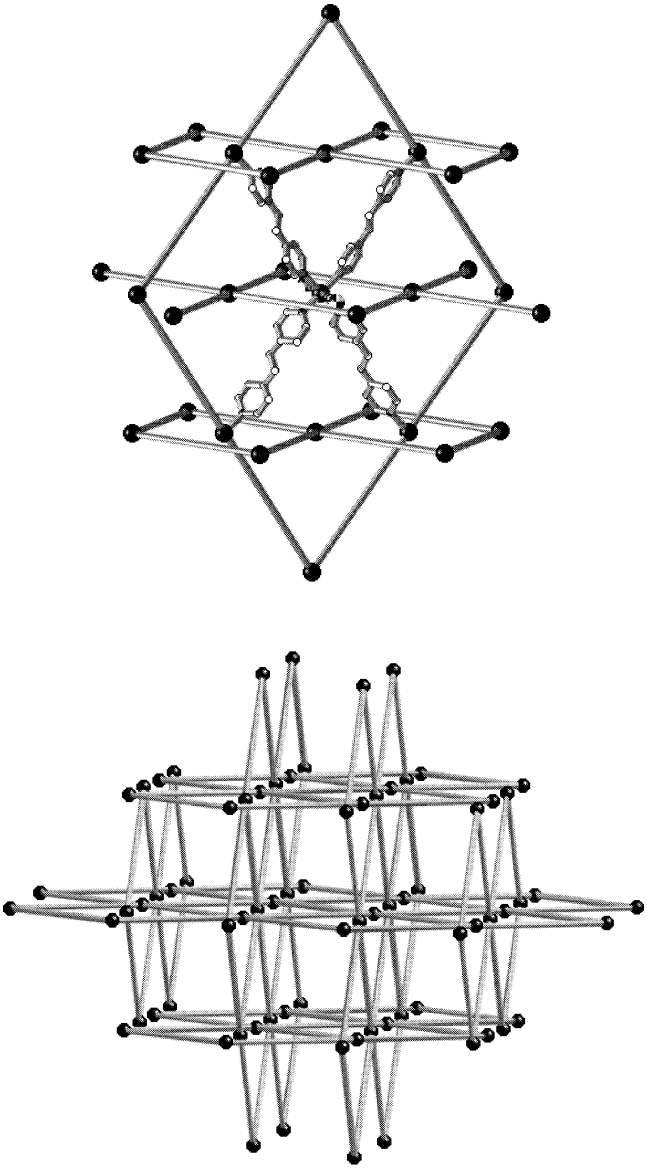

Fig. 24. Schematic views of the two independent interlocked mutually perpendicular sets of $[Fe(bpe)_2(NCS)_2]_n$ planes. The rods represent the bpe ligands connecting two iron atoms.

The suitability of bis-monodentate ligands like pyrazine (pz), bispyridylethylene (bpe) and 1,4-bis(4-pyridyl-butadiine) (bpb) has been also investigated more recently in order find out alternative approaches to obtain new 2D polymeric spin crossover compounds (Scheme 6). The compound $[Fe(pz)_2(NCS)_2]$ is made up of parallel sheets each consisting of an infinite square array of iron atoms bridged by bis-monodentate pz ligands with thiocyanato anions above and below $[Fe(pz)_2]_n$ grid-sheets achieving the pseudo-octahedral configuration around each iron atom (Fig. 22). The sheets alternate so that the iron atoms of one sheet lie vertically above and below the centres of the squares formed by the iron atoms of adjacent sheets. The coordination geometry about each iron atom is that of a tetragonally compressed octahedron. The four Fe–N(pz) basal plane bond distances, 2.246(2) Å, are significantly larger than the axial Fe–N(CS) bond distances (2.071(2) Å). The magnetic behaviour indicates that $[Fe(pz)_2(NCS)_2]$ is a 2D-antiferromagnet and consequently no spin transition occurs in this compound even at 1 GPa [73].

The compound $[Fe(bpe)_2(NCS)_2]$ MeOH is unusual in that it is made up of interlocking 2D networks constituted by parallel layers [74]. As in the previous example, the iron atom lies in a compressed octahedron with two *trans*-thiocyanato ligands filling the axial positions and four pyridine nitrogen atoms building the basal plane. Each bpe ligand connects two iron atoms defining the edges of a $[Fe]_4$ rhombus (Fig. 23). The edge-shared rhombuses define the grid-layered structures mentioned above with all the iron atoms in

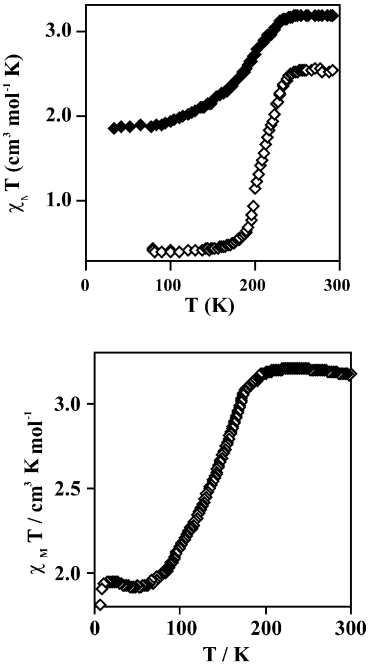

Fig. 25. Magnetic properties of $[Fe(bpe)_2(NCS)_2]CH_3OH$ (top) and $[Fe(bpb)_2(NCS)_2]\cdot 1/2CH_3OH$ (bottom).

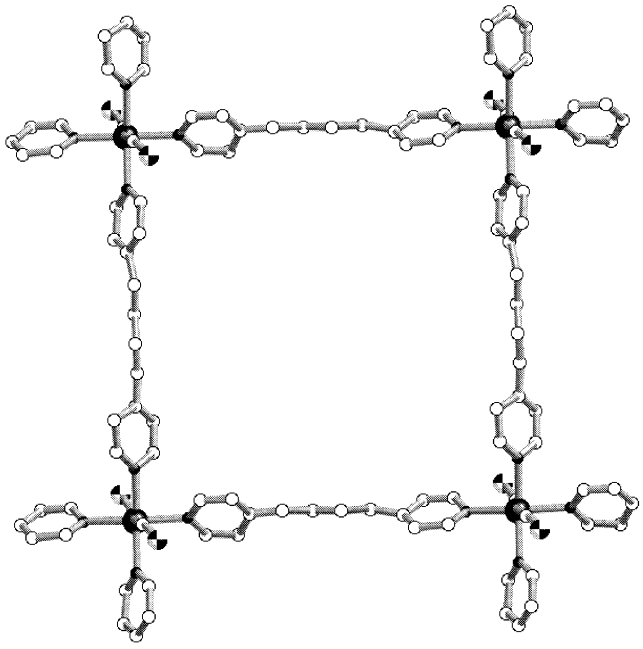

Fig. 26. Molecular structure of $[Fe(bpb)_2(NCS)_2]\cdot 1/2CH_3OH$.

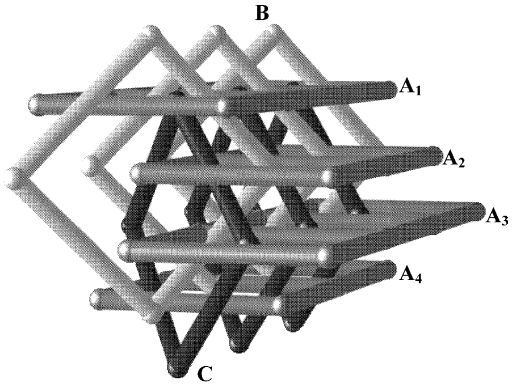

Fig. 27. Schematic view of the triple interpenetration of the $[Fe(bpb)_2(NCS)_2]_n$ grids, The parallel A set of planes, defined by the iron atoms of the type Fe1, is interpenetrated by the mutually interpenetrated B and C sets of planes, which are defined by the iron atom pf the type Fe2 (see text).

a coplanar sheet. Parallel sheets are displaced so that the iron centres of the first sheet are vertically above the third, fifth and further odd-numbered sheets, while vertically above the mid-points of $[Fe]_4$ rhombuses of the even-numbered sheets. An equivalent stack of sheets is found in planes perpendicular to the first set defining large square channels where MeOH molecules are located (Fig. 24). The magnetic properties of microcrystalline powders show that the cooperative nature of the spin conversion is very sensitive to sample preparation showing different HS and LS residual fractions at low and high temperatures, respectively. In addition, single crystals lose MeOH molecules easily and crack making the spin transition less complete (Fig. 25).

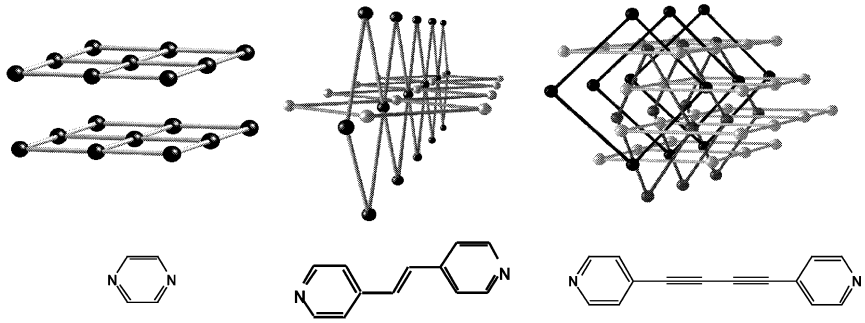

Fig. 28. Different degrees of interpenetration in the 2D (4,4) nets. No interpenetration (pz, left), double interpenetration (bpe, centre), and triple interpenetration (bpb, right).

The compound $[Fe(bpb)_2(NCS)_2]$ 0.5MeOH consists of two different arrays of nets. Two crystallographic independent iron sites (Fe1 and Fe2) define the nodes of the nets [75]. The iron atoms present similar coordination surroundings in both sites, which consist, as in precedent instances, of compressed octahedrons with two *trans*-thiocianato ligands in the axial positions and four pyridine N-atoms in the basal plane. Each bpb ligand connects two iron atoms defining large [Fe4] squares (Fig. 26). The edge-shared squares define the net structures with all the iron atoms, either coplanar (A set, Fe1) or slightly corrugated (B set, Fe2). The iron-to-iron separation through bpb ligand is 16.628 and 16.393 Å for the A and B nets, respectively. A is made up of an array of parallel sheets stacked along the [001] direction. The sheets are slipped so that they form sequences of four non super-imposable sheets per unit cell. B consists of two mutually perpendicular stacks of inter-locked squared grids organised along [110] and [−110] directions. These two stacks also interpenetrate the A set giving an unprecedented supramolecular architecture formed by three mutually perpendicular interpenetrated nets (Fig. 27). This compound undergoes a poor cooperative 50% spin transition (Fig. 25). The 50% spin conversion in this compound can be related to the presence of two iron(II) sites in the crystal. The Fe1 site is prone to undergo spin conversion as it exhibits metal-to-ligand bond distances that are slightly shorter than those of site Fe2.

Certainly, this series of compounds, based on pyridine-like ligands, is disappointing from the viewpoint of cooperativity as their spin conversions are rather incomplete and continuous (bpe and bpb derivatives). However, if we consider the complementary aspect of their structural chemistry we are faced with an interesting trend, which relates the degree of catenation in (4,4) 2D coordination polymers and the ligand size. The pz derivative shows no interpenetration of the 2D nets, and the bpe and bpb derivatives show double and triply interlocked 2D nets, respectively (Fig. 28).

A new approach to obtain novel polymeric spin crossover compounds was defined by Kitazawa et al. [76] 6 years ago when the 2D coordination polymer $\{Fe(py)_2[Ni(CN)_4]\}$ was reported. In this system the $[Ni(CN)_4]_2^-$ group acts as an anionic ligand complex in the same fashion as NCS^- or $NCSe^-$ do in many iron(II) spin crossover compounds. The main difference is its ability to allow polymerisation in two dimensions. $\{Fe(py)_2[Ni(CN)_4]\}$ is a modification of a relevant class of compounds known as Hofmann clathrate compounds and consists of 2D extended metal cyanide sheets constructed by the alternate linkage between square-planar Ni(II) and octahedral Fe(II) ions through cyano bridges. The iron(II) ion is octahedrally coordinated by four terminal N atoms of the cyano groups and two N atoms of two py ligands in *trans* configuration (Fig. 29). $\{Fe(py)_2[Ni(CN)_4]\}$ undergoes a cooperative spin transition between 210 and 170 K. The derivatives $[M(CN)_4]^{2-}$ where M = Pd, and Pt [77] have been reported recently to have a similar magnetic behaviour to the Ni derivative (see Section 4.3).

4.3. Three-dimensional coordination polymers

The possibility of investigating the cooperative effects in three-dimensional (3D) coordination spin crossover polymers has been realised recently. García et al. have reported the first 3D spin crossover polymer, which is based on the btr ligand [78]. This compound, formulated $[Fe(btr)_3](ClO_4)_2$, is closely related to the 2D $[Fe(btr)_2(NCS)_2]$ H_2O compound. The formal replacement of two thiocyanato anions in the latter by two additional bridging btr ligands affords the $[Fe(btr)_3]^{2+}$ net and changes the character of the polymeric system from 2D to 3D (Fig. 30). The crystal structures of these compounds reveals the existence of two slightly different sites for the iron(II) atoms also detected by means of Mössbauer spectroscopy. The magnetic behaviour is also sensitive to the occurrence of two sites showing the occurrence of a two-step spin transition at $T_{c1} \approx 183.5$ K and $T_{c2} \approx 222$ K. Following a similar strategy, Koninsbruggen et al. have recently reported a new 3D polymeric spin transition compound based on the ligand 1,4-

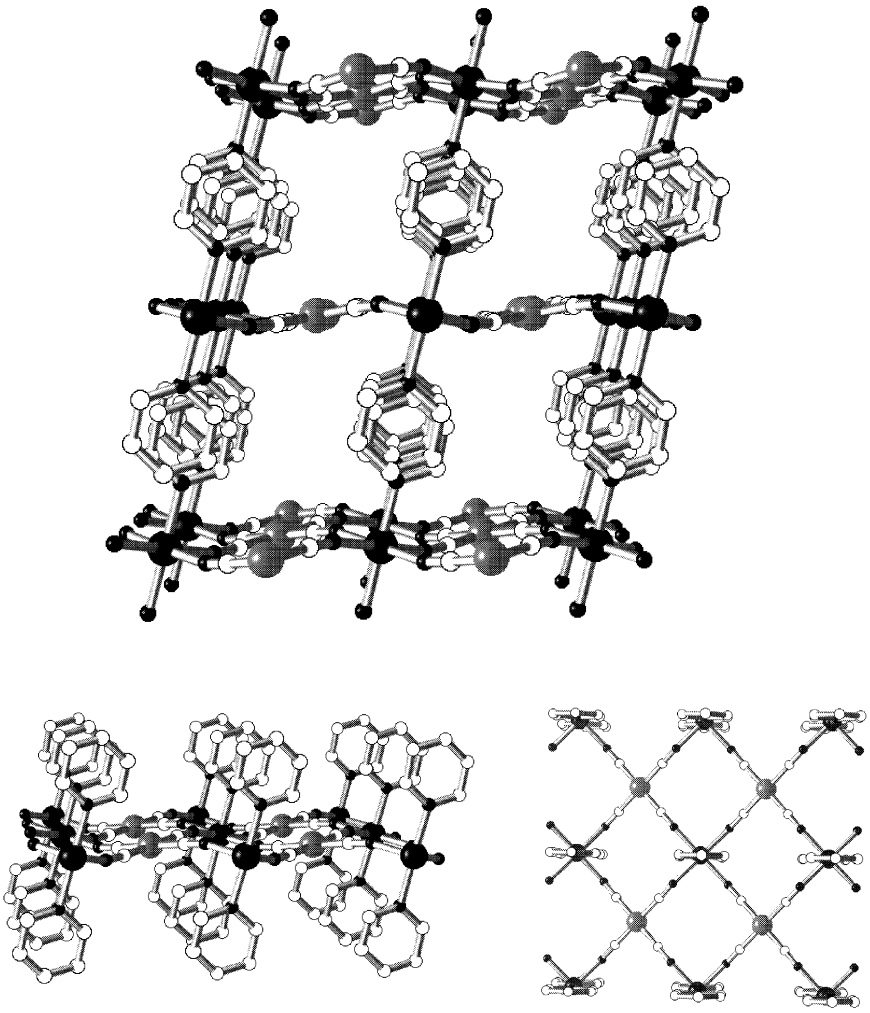

Fig. 29. Different perspectives of the polymeric structure of $\{Fe(py)_2[Ni(CN)_4]\}$. Top, two consecutive sheets, centre, side view of a sheet, and bottom top view of a sheet.

bis-tetrazol-1-yl)butane-N1,N1′ (btzb) $[Fe(btzb)_3](ClO_4)_2$ [79].

A new series of 3D spin crossover compounds has been realised from the $\{Fe(py)_2[M(CN)_4]\}$ 2D system (M is Ni(II), Pd(II) or Pt(II)) and recently reported by Niel et al. [77]. Replacement of the py ligand by pz ligand in the 2D system affords the new family of 3D compounds $\{Fe(pz)[M(CN)_4]\}2H_2O$. In this new structure the pz ligand bridges the iron atoms of consecutive sheets achieving a pillaring of the 2D sheets by vertical columns of the pz bridge to give the 3D structure (Fig. 31). The magnetic properties of the pairs of compounds, [FeLM], are compared in Fig. 32. The 3D compounds undergo strong cooperative spin transitions with 20–40 K width hysteresis loops. In the case of the py derivatives the hysteresis has a maximum of 9 K width. The significantly higher T_c values observed for the pz derivatives compared with their py counterparts cannot be explained in terms of ligand field theory as py imparts a stronger ligand field than pz. Thus, the internal pressure originated from the more rigid 3D structures may be responsible for the effective stronger ligand field at iron(II) site. This example is particularly suitable to illustrate how the change of dimensionality from 2D to 3D in two tightly related systems influences cooperativity.

5. Conclusion and outlook

In the first part of this paper we have illustrated that it is possible to rationalise qualitatively the character of the spin transition through careful structural investigation. From the structural data it can be inferred that the $[FeN_6]$ chromophore and its change upon spin conversion are found to be similar for all iron(II) compounds. Consequently, it cannot play any influence on the spin crossover regime in the $[Fe(L)_2(NCS)_2]$ family. In fact,

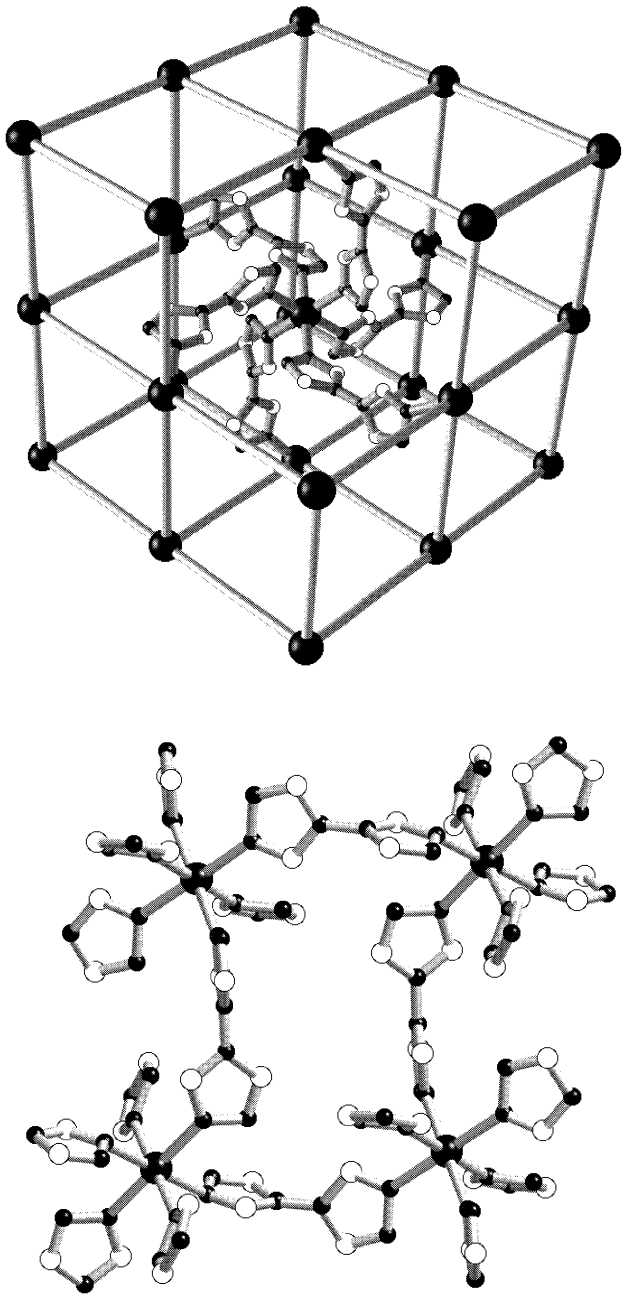

Fig. 30. Representation of the connectivity between iron atoms (top), and a fragment of a square grid (bottom) of the polymeric 3D structure of the cation $[Fe(btr)_3]^{2+}$.

the key factor governing the cooperative nature of the spin change in this series of mononuclear compounds is related to the number and strength of intermolecular interactions, which spread to the whole crystal the intramolecular structural modifications. We have pointed out that this propagation can be tuned playing with the nature of the ligands coordinated to the active site, for instance, increasing the aromatic nature of the ligand from btz to dpp. Of course, other kinds of intermolecular interactions, like hydrogen bonding or

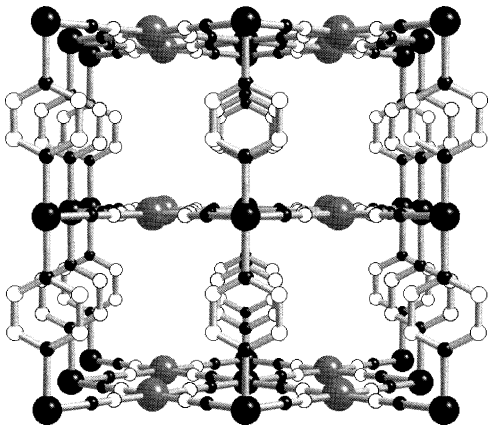

Fig. 31. Perspective view of the 3D coordination polymer $\{Fe(pz)[Pt(CN_4]\}\cdot 2H_2O$.

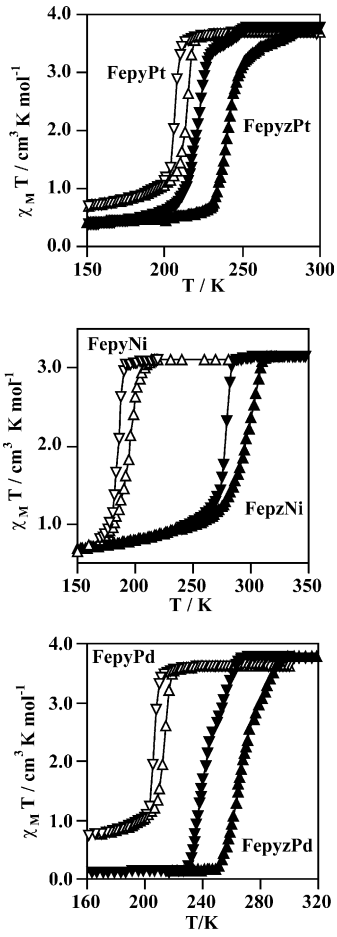

Fig. 32. Magnetic properties of $\{Fe(L)_x[M(CN)_4]\}\cdot nS$ where L = py (x = 2), and L = pz (x-1, nS = $2H_2O$.

specific atomic interactions, can strongly influence the cooperative nature of the spin conversion.

The through bipyrimidine iron coupled dinuclear compounds have revealed the occurrence of a rich variety of spin crossover behaviour. The most remarkable feature is the occurrence of the spin conversion in

two steps which corresponds to the existence of three types of spin pairs: [LS–LS], [LS–HS], and [HS–HS]. The stabilisation of the spin mixed pair stems from the synergistic interplay between anticooperative intramolecular interactions stabilising the spin mixed pairs and cooperative intermolecular interactions stabilising spin like pairs. The real existence and reliability of the [LS–HS] spin pairs have been established by means of thermal, pressure, and light induced spin conversion monitored from magnetic and field dependent Mössbauer techniques.

Polymeric spin crossover compounds represent a relatively new approach to investigating new strong cooperative regimes. Presently, the reported examples concerning polymeric compounds are greatly limited to a small number. Despite this, it can be inferred, from the examples herein reviewed, that by connecting the active sites with appropriate rigid bridging ligands it is possible to obtain materials with sharp responses and large hysteresis (memory effect). We believe that the synthesis of new 1-3D polymeric spin crossover compounds will require an imaginative effort and that much inspiration will arise from the huge stock of knowledge of metallo-supramolecular chemistry generated during the last 15 years.

An important question concerning the spin crossover phenomenon is connected with the desire to synthesise new kinds of supramolecular functional materials. It could be achieved combining the unique properties of spin crossover phenomenon with other physical properties like cooperative magnetic ordering, which could afford new interesting switching molecular materials. In addition to these electronic properties, the mechanical properties associated to the spin change should also be a motive of inspiration in molecular design of artificial molecular systems with allosteric responses [80]. Biological systems are usually paradigms that guide the work of synthetic chemists aiming to create chemical analogues of these complex natural structures. In this regard, Perutz et al. have stated "*Haemoglobin may be unique in exploiting changes in Fe–N bond lengths accompanying the transition from high-spin to low-spin ferrous iron for the purpose of efficient oxygen transport: without use of that spin transition fast-moving animals could not have evolved*" [9]. We are convinced that haemoglobin will represent an unavoidable model for future research in supramolecular functional materials based on the spin crossover phenomenon.

Acknowledgements

We are grateful for financial support from the European Commission through the TMR-Network project "Thermal and Optical Switching of Spin States (TOSS)", Contract No. ERB-FMRX-CT98-0199EEC/TMR. Some important results here reviewed have been carried out in collaboration with other TOSS groups, in particular, pressure and Mössbauer experiments in presence of strong magnetic combined with LIESST effect, were performed together with Professor P. Gütlich and Dr. V. Ksenovontov and photomagnetic measurements with Professor O. Kahn and Dr. J.F. Létard to whom we are deeply grateful. We thank the financial assistance from the Ministerio Español de Ciencia y Tecnología (project BQU 2001-2928).

References

[1] J.M. Lehn, Supramolecular Chemistry, VCH, Weinheim, 1995.
[2] C.N.R. Rao, Acc. Chem. Rev. 17 (1984) 83.
[3] C.N.R. Rao, J. Gopalakrishnan, New Directions in Solid State Chemistry, Cambridge Solid State Sciences Series, Cambridge University Press, 1986.
[4] P. Gütlich, A. Hauser, H. Spiering, Angew. Chem. Int. Ed. Engl. 33 (1994) 2024.
[5] E. König, Struct. Bonding (Berlin) 76 (1991) 51.
[6] E. König, Prog. Inorg. Chem. 35 (1987) 527.
[7] H. Spiering, T. Kohlhaas, H. Romstedt, A. Hauser, C. Bruns-Yilmaz, J. Kusz, P. Gütlich, Coord. Chem. Rev. 190–192 (1999) 629.
[8] A. Hauser, J. Jeftic, H. Romstedt, R. Hinek, H. Spiering, Coord. Chem. Rev. 190–192 (1999) 471.
[9] M.F. Perutz, G. Fermi, B. Luisi, B. Shaanan, R.C. Liddington, Acc. Chem. Res. 20 (1987) 309.
[10] B. Gallois, J.A. Real, C. Haw, J. Zarembowitch, Inorg. Chem. 20 (1990) 1152.
[11] M. Konno, M. Mikami-Kido, Bull. Chem. Soc. Jpn. 64 (1991) 339.
[12] J.A. Real, B. Gallois, T. Granier, F. Suez-Panamá, J. Zarembowitch, Inorg. Chem. 31 (1992) 4972.
[13] J.A. Real, M.C. Muñoz, E. Andrés, T. Granier, B. Gallois, Inorg. Chem. 33 (1994) 3587.
[14] A. Ozarowski, B.R. McGarvey, A.B. Sarkar, J.E. Drake, Inorg. Chem. 27 (1988) 628.
[15] J.F. Létard, S. Montant, P. Guionneau, P. Martin, A. Le Calvez, E. Freysz, D. Chasseau, R. Lapouyade, O. Kahn, J. Chem. Soc. Chem. Commun. (1997) 745.
[16] J.F. Létard, P. Guionneau, E. Codjovi, O. Lavastre, G. Bravic, D. Chasseau, O. Kahn, J. Am. Chem. Soc. 119 (1997) 10861.
[17] P. Guionneau, J.F. Létard, D.S. Yufit, D. Chasseau, G. Bravic, A.E. Goeta, J.A.K. Howard, O. Kahn, J. Mater. Chem. 9 (1999) 985.
[18] Z.J. Zhong, J.Q. Tao, Z. Yu, C.Y. Dun, Y.J. Liu, X.Z. You, J. Chem. Soc. Dalton Trans. (1998) 327.
[19] N. Moliner, M.C. Muñoz, S. Létard, J.F. Létard, X. Solans, R. Burriel, M. Castro, O. Kahn, J.A. Real, Inorg. Chim. Acta 291 (1999) 279.
[20] W.A. Baker, H.M. Bobonich, Inorg. Chem. 3 (1964) 1184.
[21] E. König, K. Madeja, Chem. Commun. 3 (1967) 61.
[22] A.T. Casey, Aust. J. Chem. 21 (1968) 2291.
[23] E. Köning, K. Madeja, K.J. Watson, J. Am. Chem. Soc. 90 (1968) 1146.
[24] G. Bradley, V. McKee, S.M. Nelson, J. Chem. Soc. (1978) 522.
[25] E. König, K. Madeja, Inorg. Chem. 6 (1967) 48.
[26] P. Gütlich, Struct. Bonding (Berlin) 44 (1981) 83.
[27] T. Granier, B. Gallois, J. Gaultier, J.A. Real, J. Zarembowitch, Inorg. Chem. 32 (1993) 5305.

[28] L. Wiehl, G. Kiel, C.P. Köhler, H. Spiering, P. Gütlich, Inorg. Chem. 25 (1986) 1565.
[29] S. Usha, R. Srinivasan, C.N.R. Rao, Chem. Phys. 100 (1985) 447.
[30] C. Roux, J. Zarembowitch, J.P. Itié, A. Polian, M. Verdaguer, R. Claude, E. Dartyge, A. Fontaine, E. Tolentino, Inor. Chem. 30 (1991) 3174.
[31] C.P. Köhler, R. Jakobi, E. Meissner, L. Wiehl, H. Spiering, P. Gütlich, J. Phys. Chem. Solids 51 (1990) 239.
[32] E.V. Dose, L.J. Wilson, Inorg. Chem. 17 (1978) 2660.
[33] G. Brewer, E. Sinn, Inorg. Chem. 24 (1985) 4580.
[34] M. Julve, G. de Munno, G. Bruno, M. Verdaguer, Inorg. Chem. 27 (1988) 3160.
[35] M. Julve, M. Verdaguer, G. de Munno, J.A. Real, G. Bruno, Inorg. Chem. 32 (1999) 795.
[36] I. Castro, M. Julve, G. de Munno, G. Bruno, J.A. Real, F. Lloret, J. Faus, J. Chem. Soc. Dalton Trans. (1992) 1739.
[37] J.A. Real, G. de Munno, R. Chiappetta, M. Julve, F. Lloret, Y. Journaux, J.C. Colin, G. Blondin, Angew. Chem. Int. Ed. Engl. 33 (1994) 1184.
[38] G. de Munno, M. Julve, in: N. Ruso, D.R. Salahub (Eds.), Metal–Ligand Interactions, Kluwer, 1996, p. 139.
[39] E. Andrés, G. de Munno, M. Julve, J.A. Real, F. Lloret, J. Chem. Soc. Dalton Trans. (1993) 2169.
[40] J.A. Real, J. Zarembowitch, O. Kahn, X. Solans, Inorg. Chem. 26 (1987) 2939.
[41] A.B. Gaspar, M.C. Muñoz, J.A. Real, unpublished results.
[42] J.A. Real, H. Bolvin, A. Bousseksou, A. Dworkin, O. Kahn, F. Varret, J. Zarembowitch, J. Am. Chem. Soc. 114 (1992) 4650.
[43] J.A. Real, I. Castro, A. Bousseksou, M. Verdaguer, R. Burriel, M. Castro, J. Linares, F. Varret, Inorg. Chem. 36 (1997) 455.
[44] V. Ksenofontov, A.B. Gaspar, J.A. Real, P. Gütlich, J. Phys. Chem. B 105 (2001) 12266.
[45] V. Ksenofontov, H. Spiering, S. Reiman, Y. García, A.B. Gaspar, N. Moliner, J. Real, P. Gütlich, Chem. Phys. Lett. 348 (2001) 381.
[46] S. Decurtins, P. Gütlich, C.P. Köhler, H. Spiering, A. Hauser, Chem. Phys. Lett. 105 (1984) 1.
[47] A. Hauser, Chem. Phys. Lett. 124 (1986) 543.
[48] J.F. Létard, J.A. Real, N. Moliner, A.B. Gaspar, L. Capes, O. Cador, O. Kahn, J. Am. Chem. Soc. 121 (1999) 10630.
[49] G. Chastanet, A.B. Gaspar, J.A. Real, J.F. Létard, Chem. Commun. (2001) 819.
[50] L.G. Lavrenova, V.N. Ikorskii, V.A. Varnek, I.M. Oglezneva, S.V. Larionov, Koord. Khim. 12 (1986) 207.
[51] L.G. Lavrenova, V.N. Ikorskii, V.A. Varnek, I.M. Oglezneva, S.V. Larionov, J. Struct. Chem. 34 (1993) 960.
[52] K.H. Sugiyarto, H.A. Goodwin, Aust. J. Chem. 47 (1994) 263.
[53] J. Kröber, E. Codjovi, O. Kahn, F. Grolière, C. Jay, J. Am. Chem. Soc. 115 (1993) 9810.
[54] L.G. Lavrenova, N.G. Yudina, V.N. Okorskii, V.A. Varnek, I.M. Oglezneva, S.V. Larionov, Polyhedron 14 (1995) 1333.
[55] V.A. Varnek, L.G. Lavrenova, J. Struct. Chem. 36 (1995) 104.
[56] E. Codjovi, L. Sommier, O. Kahn, C. jay, New J. Chem. 20 (1996) 503.
[57] O. Kahn, C.J. Martinez, Science 279 (1998) 44.
[58] A. Michalowicz, J. Moscovici, B. Ducourant, D. Gracco, O. kahn, Chem. Mater. 7 (1995) 1833.
[59] P.J. van Koningsbruggen, Y. Garcia, O. Kahn, L. Founès, H. Kooijman, A.L. Spek, J.G. Haasnoot, J. Moscovici, K. Provost, A. Michalowicz, F. Renz, P. Gütlich, Inorg. Chem. 39 (2000) 1891.
[60] G. de Munno, M. Julve, J.A. Real, F. lloret, R. Scopelliti, Inorg. Chim. Acta 250 (1996) 81.
[61] N. Moliner, M.C. Muñoz, J.A. Real, Inorg. Chem. Commun. 2 (1999) 25.
[62] S. Noro, M. Kondo, T. Ishii, S. Kitagawa, H. Matsuzaka, J. Chem. Soc. Dalton Trans. (1999) 1569.
[63] J. Lu, T. Paliwala, S.C. Lim, C. Yu, T. Niu, A.J. Jacobson, Inorg. Chem. 36 (1997) 923.
[64] N. Moliner, M.C. Muñoz, J.A. Real, unpublished results.
[65] J.G. Haasnoot, Coord. Chem. Rev. 200–202 (2000) 131.
[66] D.W. Engelfriet, G.C. Verschoor, Acta Crystallogr. Sect. B 37 (1981) 237.
[67] J.G. Haasnoot, W.L. Groeneveld, Z. Naturforsch. 34b (1979) 1500.
[68] B. van der Griendt, J.G. Haasnoot, J. Reedijk, L.J. de Jongh, Chem. Phys. Lett. 111 (1984) 161.
[69] W. Vreugdenhill, J.H. van Diemen, R.A.G. de Graaff, J.G. Haasnoot, J. Reedijk, A.M. van der Kraan, O. Kahn, J. Zarembowitch, Polyhedron 9 (1990) 2971.
[70] J.P. Martin, J. Zarembowitch, A. Dworkin, J.G. Haasnoot, E. Codjovi, Inorg. Chem. 33 (1994) 2617.
[71] E. Codjovi, N. Menéndez, J. Jeftic, F. Varret, C.R. Acad. Sci. Paris Chim. 4 (2001) 181.
[72] Y. Garcia, V. Ksenofontov, G. Levchenko, G. Schmitt, P. Gütlich, J. Phys. Chem. B 104 (2000) 5045.
[73] J.A. Real, G. de Munno, M.C. Muñoz, M. Julve, Inorg. Chem. 30 (1991) 2701.
[74] J.A. Real, E. Andrés, M.C. Muñoz, M. Julve, T. Granier, A. Bousseksou, F. Varret, Science 268 (1995) 265.
[75] N. Moliner, M.C. Muñoz, S. Létard, X. Solans, N. Menéndez, A. Goujon, F. Varret, J.A. real, Inorg. Chem. 39 (2000) 5390.
[76] T. Kitazawa, Y. Gomi, M. Takahashi, M. Takeda, M. Enemoto, A. Miyazaki, T. Enoki, J. Mater. Chem. 6 (1996) 119.
[77] V. Niel, J.M. Martínez-Agudo, M.C. Muñoz, A.B. Gaspar, J.A. Real, Inorg. Chem. 40 (2001) 3838.
[78] Y. Garcia, O. Kahn, L. Rabardel, B. Chansou, L. Salmon, J.P. Tuchagues, Inorg. Chem. 38 (1999) 4663.
[79] P.J. van Koningsbruggen, Y. Garcia, H. Kooijman, A.L. Spek, J.G. Haasnoot, O. Kahn, J. Linares, E. Codjovi, F. Varret, J. Chem. Soc. Dalton Trans. (2001) 466.
[80] M. Takeuchi, M. Ikeda, A. Sugasaki, S. Shinkai, Acc. Chem. Res. 34 (2001) 865.